

ISTANBUL TECHNICAL UNIVERSITY ★ GRADUATE SCHOOL OF SCIENCE
ENGINEERING AND TECHNOLOGY

**SYNTHESIS AND CHARACTERIZATION OF CROSS-LINKED
POLY (DIMETHYL SILOXANE) NANOCOMPOSITES**

M.Sc. THESIS

Yağmur ÇAVUŞOĞLU
(515111024)

Department of Polymer Science and Technology

Polymer Science and Technology Programme

JANUARY 2013

ISTANBUL TECHNICAL UNIVERSITY ★ GRADUATE SCHOOL OF SCIENCE
ENGINEERING AND TECHNOLOGY

**SYNTHESIS AND CHARACTERIZATION OF CROSS-LINKED
POLY (DIMETHYL SILOXANE) NANOCOMPOSITES**

M.Sc. THESIS

Yağmur ÇAVUŞOĞLU
(515111024)

Department of Polymer Science and Technology

Polymer Science and Technology Programme

Thesis Advisor : Prof. Dr. Nurseli UYANIK
Co-Advisor : Assoc. Prof. Dr. Güralp ÖZKOÇ

JANUARY 2013

İSTANBUL TEKNİK ÜNİVERSİTESİ ★ FEN BİLİMLERİ ENSTİTÜSÜ

**ÇAPRAZ BAĞLI POLİ (DİMETİL SİLOKSAN)
NANOKOMPOZİTLERİN SENTEZİ VE KARAKTERİZASYONU**

YÜKSEK LİSANS TEZİ

**Yağmur ÇAVUŞOĞLU
(515111024)**

Polimer Bilim ve Teknolojileri

Polimer Bilim ve Teknolojileri Programı

**Tez Danışmanı : Prof. Dr. Nurseli UYANIK
Eş-Danışmanı : Doç. Dr. Güralp ÖZKOÇ**

OCAK 2013

Yağmur ÇAVUŞOĞLU, a **M.Sc.** student of **ITU Graduate School of Science Engineering and Technology** student ID **515111024**, successfully defended the thesis entitled “**SYNTHESIS AND CHARACTERIZATION OF CROSS-LINKED POLY (DIMETHYL SILOXANE) NANOCOMPOSITES**”, which she prepared after fulfilling the requirements specified in the associated legislations, before the jury whose signatures are below.

Thesis Advisor : **Prof. Dr. Nurseli UYANIK**
İstanbul Technical University

Co-advisor : **Assoc. Prof. Dr. Güralp ÖZKOÇ**
Kocaeli University

Jury Members : **Prof. Dr Nurseli UYANIK**
İstanbul Technical University

Assoc. Prof. Dr. Güralp ÖZKOÇ
Kocaeli University

Prof. Dr. Nilgün Köken KIZILCAN
İstanbul Technical University

Prof. Dr. Ahmet AKAR
İstanbul Technical University

Prof. Dr. Ayfer SARAÇ
Yıldız Technical University

Date of Submission : 17 December 2012

Date of Defense : 24 January 2013

To my mother,

FOREWORD

Words stay short at expressing my sincere appreciation and gratitude to my thesis supervisor, Prof. Dr. Nurseli UYANIK for her infinite support, guidance and helpful suggestions throughout my research. It was a great honor and pleasure to work with her and benefit from her experience.

I also would like to endless thank my co-advisor Assoc. Prof. Dr. Güralp ÖZKOÇ from Kocaeli University, Department of Chemical Engineering. I cannot even imagine any study without his support, invaluable advice and endless guidance. Also thanks to him for providing me an opportunity to make my experimental studies at Kocaeli University, Polymer Laboratory.

I would like to thank Eczacıbaşı Esan Company for their material support Bentonite.

I also would like to thank Mehmet KODAL from Kocaeli University Köseköy Vocational College providing me to make my tensile tests.

I also would like to thank Efgan KİBAR from Kocaeli University providing me to make X-Ray Diffraction (XRD).

I would like to thank Dilek TURAN and Şerif ERDOĞAN/R&D Manager from Elastron Kimya A.Ş. for providing me to make Thermogravimetric Analyses (TGA).

I would like to thank Prof. Dr. Yusuf MENCELOĞLU from Sabancı University providing me opportunity Field Emission Scanning Electron Microscopy (FE-SEM) tests.

Most of all, I especially would like to thank my family, my mother Saniye ÇAVUŞOĞLU, my father Seyit ÇAVUŞOĞLU and my sister Merve ÇAVUŞOĞLU for supporting me all my life.

My personal thanks are to Asist. Şebnem Kemaloğlu DOĞAN, Asist. N.Gamze KARSLI, Hümeysra ŞİRİN, Sibel YILDIZ, Asist. Filiz Uğur NİĞİZ from Kocaeli University and Türker DUYAR, Gül CAN, Hale TOZLU, Asist. Merve Çetintaş MOCAN, Merve ZAKUT from ITU for their friendly manner.

January 2013

Yağmur ÇAVUŞOĞLU

Chemical Engineer

TABLE OF CONTENTS

	<u>Page</u>
FOREWORD	ix
TABLE OF CONTENTS	xi
ABBREVIATIONS	xiii
LIST OF TABLES	xv
LIST OF FIGURES	xvii
SUMMARY	xxi
ÖZET	xxiii
1. INTRODUCTION	1
2. THEORETICAL PART	3
2.1 Composite Materials	3
2.1.1 Polymer matrix composites	4
2.2 Nanocomposites	5
2.2.1 Polymer-layered silicate nanocomposites	6
2.2.2 Structure of layered silicates	6
2.2.2.1 Bentonite	7
2.2.2.2 Organic modification of bentonite	8
2.2.3 Nanocomposite preparation techniques	10
2.2.3.1 In-Situ polymerization method	10
2.2.3.2 Solution intercalation method	11
2.2.3.3 Melt mixing method	12
2.3 Polysiloxanes	13
2.3.1 Linear siloxanes	15
2.3.2 Cyclic siloxanes	16
2.4 Cross-linking of Poly (dimethyl siloxane) (PDMS)	16
2.4.1 Cross-linking with radicals	17
2.4.2 Cross-linking by condensation	17
2.4.3 Cross-linking by addition	19
2.5 Literature Overview of Siloxane Nanocomposites	20
3. EXPERIMENTAL	25
3.1 Chemicals	25
3.1.1 Poly (dimethyl siloxane) (PDMS)	25
3.1.2 Bentonite	25
3.1.3 Hexadecyltrimethylammonium chloride (HDTMAC)	25
3.1.4 (4-Carboxybutyl) triphenylphosphonium bromide (4CBTPPB)	25
3.1.5 Tributylhexadecylphosphonium bromide (TBHDPB)	25
3.1.6 Dicumyl peroxide	25
3.1.7 Toluene	26
3.1.8 Chloroform	26

3.2 Equipments.....	26
3.2.1 Magnetic stirrer with heater	26
3.2.2 Vacuum oven	26
3.2.3 Ultrasonic bath	26
3.2.4 Fourier transform infrared spectroscopy (FTIR) test device	26
3.2.6 Thermogravimetric analysis (TGA) test device.....	26
3.2.7 Mechanical test device	27
3.2.8 Dynamic mechanical analysis (DMA) test device	27
3.2.9 Shore-A hardness test device	27
3.2.10 Contact angle test device	27
3.2.11 Field emission-scanning electron microscopy (FE-SEM) test device..	27
3.3 Experimental Procedure.....	27
3.3.1 Modification of bentonite	27
3.3.2 PDMS nanocomposites preparation	28
3.4 Characterization.....	28
3.4.1 Fourier transform infrared spectroscopy (FTIR)	28
3.4.2 X-ray diffraction (XRD) analysis.....	28
3.4.3 Thermogravimetric analysis (TGA)	29
3.4.4 Tensile test	29
3.4.5 Dynamic mechanical analysis (DMA)	29
3.4.6 Shore-A hardness test	29
3.4.7 Contact angle measurements	29
3.4.8 Field emission-scanning electron microscopy (FE-SEM).....	30
4. RESULTS AND DISCUSSION	31
4.1 FTIR Results	32
4.2 XRD Analysis Results	34
4.3 TGA Results.....	37
4.4 Tensile Test Results.....	42
4.5 DMA Test Results	44
4.6 Hardness Test Results.....	48
4.7 Contact Angle Test Results	49
4.8 FE-SEM Test Results	50
5. CONCLUSION	53
REFERENCES	55
CURRICULUM VITAE.....	59

ABBREVIATIONS

PDMS	: Poly (dimethyl siloxane)
HDTMAC	: Hexadecyltrimethylammonium chloride
4CBTPPB	: (4-Carboxybutyl) triphenylphosphonium bromide
TBHDPB	: Tributylhexadecylphosphonium bromide
MMT	: Montmorillonite
UV	: Ultra Violet
KPa	: Kilo Pascal
MPa	: Mega Pascal
TEOS	: Tetraethyl orthosilicate
OMMT	: Organically modified montmorillonite
PV	: Pervaporation
SEM	: Scanning Electron Microscopy
FTIR	: Fourier Transform Infrared Spectroscopy
XRD	: X-ray Diffraction
TGA	: Thermal Gravimetric Analysis
ASTM	: American Society for Testing and Materials
AFM	: Atomic Force Microscopy
IPA	: Isopropanol
CEC	: Cation Exchange Capacity

LIST OF TABLES

	<u>Page</u>
Table 2.1 : Chemical formulas of commonly used smectite type layered silicates	7
Table 2.2 : Properties of PDMS.....	14
Table 4.1 : XRD results of the pure bentonite , organoclays and PDMS/organoclay nanocomposites	35
Table 4.2 : Tensile test results of the pure PDMS and PDMS-4CBTPPB-B nanocomposite with varied contents of organoclays	42
Table 4.3 : Tensile test results of the pure PDMS and PDMS-HDTMAC-B nanocomposite with varied contents of organoclays	42
Table 4.4 : Tensile test results of the pure PDMS and PDMS-TBHDPB-B nanocomposite with varied contents of organoclays	42
Table 4.5 : Storage modulus (E') results of PDMSNCs	45
Table 4.6 : Loss modulus (E'') results of PDMSNCs	46
Table 4.7 : Absolute value of modulus ($ E $) test results odPDMSNCs.....	47

LIST OF FIGURES

	<u>Page</u>
Figure 2.1 : Structure of 2:1 phyllosilicates	7
Figure 2.2: Cation exchange process between alkylammonium ions and exchangeable cations of layered silicate structure and dynamics of polymer-layered silicate nanocomposites.	9
Figure 2.3 : Orientations of alkylammonium ions in the galleries of layered silicates: (a)monolayer, (b)bilayers, (c)pseudo-trimolecular layers and (d,e)paraffin type arrangements of alkylammonium ions with different tilting angles of the alkyl chains.	9
Figure 2.4 : Schemes of polymer/clay nanocomposites including conventional composite and nanocomposite with intercalated (i), exfoliated (ii) or cluster (iii) structure.....	10
Figure 2.5 : In-situ polymerization method.....	11
Figure 2.6 : Solution intercalation method.....	11
Figure 2.7 : Melt mixing method.....	13
Figure 2.8 : Chemical backbone structure of PDMS.....	14
Figure 2.9 : Linear siloxane structure	15
Figure 2.10 : Hexamethyl disiloxane.....	15
Figure 2.11 : Poly (dimethyl siloxane) (PDMS).	15
Figure 2.12 : Vinyl-terminated poly (dimethyl siloxane).	16
Figure 2.13 : Octamethyl cyclotetrasiloxane.....	16
Figure 4.1 : FTIR spectra of the cross-linked pure PDMS and PDMSNCs.....	33
Figure 4.2 : XRD pattern of the pure bentonite and bentonite modified with HDTMAC, TBHDPB and 4CBTPPB.....	35
Figure 4.3 : XRD pattern of the organoclay modified with HDTMAC and its PDMS/organoclay nanocomposite with 3-5-10 % contents.	36
Figure 4.4: XRD pattern of the organoclay modified with TBHDPB and its PDMS/organoclay nanocomposite with 3-5-10 % contents	36
Figure 4.5 : XRD pattern of the organoclay modified with 4CBTPPB and its PDMS/organoclay nanocomposite with 3-5-10 % contents.	36
Figure 4.6 : TGA thermograms of the pure bentonite and organically modified bentonites	37
Figure 4.7 : TGA thermogram of the cross-linked pure PDMS, PDMS-HDTMAC-B-5, PDMS-TBHDPB-B-5 and PDMS-4CBTPPB-B-5.	38
Figure 4.8 : Decomposition temperatures till the 4 % of weight loss of the materials.	38
Figure 4.9 : TGA thermogram of the PDMS-HDTMAC-B-3, PDMS-HDTMAC-B-5 and PDMS-HDTMAC-B-10	39
Figure 4.10 : Percent weight loss versus temperature comparison of the pure-PDMS, PDMS-HDTMAC-B-3, PDMS-HDTMAC-B-5 and PDMS-HDTMAC-B-10.....	39

Figure 4.11 : TGA thermogram of the PDMS-TBHDPB-B-3, PDMS-TBHDPB-B-5 and PDMS-TBHDPB -B-10	40
Figure 4.12 : Percent weight loss versus temperature comparison of the pure-PDMS, PDMS-TBHDPB-B-3, PDMS-TBHDPB-B-5 and PDMS-TBHDPB-B-10.....	40
Figure 4.13 : TGA thermogram of the PDMS-4CBTPPB-B-3, PDMS-4CBTPPB-B-5 and PDMS-4CBTPPB-B-10	41
Figure 4.14 : % Weight loss versus temperature comparison of the pure-PDMS, PDMS-4CBTPPB-B-3, PDMS-4CBTPPB -B-5 and PDMS-4CBTPPB-B-10	41
Figure 4.15 : Tensile strength results of PDMS-4CBTPPB-B, PDMS-TBHDPB-B and PDMS-HDTMAC-B with varied contents	43
Figure 4.16 : Elongation at break results of PDMS-4CBTPPB-B, PDMS-HDTMAC-B and PDMS-TBHDPB-B with varied contents	43
Figure 4.17 : Frequency versus storage modulus (E') results of PDMSNCs	45
Figure 4.18 : Frequency versus loss modulus (E'') results of PDMSNCs	46
Figure 4.19 : Frequency versus absolute value of the modulus ($ E $) results of PDMSNCs.....	47
Figure 4.20 : Hardness test results of the PDMS/organoclay nanocomposite with varied organoclay content	48
Figure 4.21 : Water contact angle results of the pure PDMS and PDMSNCs	49
Figure 4.22 : Surface free energy results of the pure PDMS and PDMSNCs	50
Figure 4.23 : FE-SEM image of PDMS-4CBTPPB-B-5	51
Figure 4.24 : FE-SEM image of PDMS-TBHDPB-B-5	51

SYNTHESIS AND CHARACTERIZATION OF CROSS-LINKED POLY (DIMETHYL SILOXANE) NANOCOMPOSITES

SUMMARY

Composite materials are a combination of two or more materials in which the constituents retain their identities. Composite structures can be classified according to the matrix material that they are made up of. One of the most widely used types of composite structure is polymer matrix composites. They are mixtures of polymers with inorganic and organic additives having certain geometries, such as fibers, flakes, spheres and particulates.

Nanocomposites are a combination of two or more phases containing different compositions or structures, where at least one of the phases is in the nanoscale regime. These materials exhibit behavior different from conventional composite materials with microscale structure, due to the small size of the structural unit and the high surface-to-volume ratio.

Polysiloxanes have unique properties for much diversified applications ranging from electrical insulation to biomaterials and to space research. Poly (dimethyl siloxanes) (PDMSs) are the most common member of the polysiloxane group. A large molar volume, a low cohesive energy density and high flexibility are the important physical properties of the PDMS. In addition, PDMS are transparent to visible and UV light, very resistant to ozone and corona discharge, stable against atomic oxygen and even oxygen plasmas. Other outstanding properties include film forming ability, high permeability to various gases, hydrophobic behavior, release action, surface activity and chemical and physiological inertness. Despite their many outstanding properties, PDMS rubbers require extremely high molecular weights to develop useful mechanical properties.

The present study was aimed to use organically modified bentonites in the cross-linked poly (dimethyl siloxane) nanocomposite (PDMSNC) preparation. The cross-linked PDMS nanocomposites were prepared by in-situ polymerization method by using alkyl ammonium and alkyl phosphonium modified bentonites with varying compositions such as 3-5-10%. The cross-linked PDMS without organoclay was also prepared for the comparison purposes. The modifiers were hexadecyltrimethylammonium chloride, tributylhexadecylphosphonium bromide and (4-carboxybutyl) triphenylphosphonium bromide. The pure cross-linked PDMS rubber and its nanocomposites were characterized by morphological, thermal and mechanical analysis. Structural analysis of the prepared organoclays and PDMS nanocomposites were determined by Fourier transform infrared spectroscopy (FTIR). The morphological investigations were performed by X-ray diffraction (XRD) and field emission-scanning electron microscopy (FE-SEM) to obtain the interlayer distance of PDMSNCs. Elastic modulus, tensile strength and elongation at break values were determined by tensile tests. Storage modulus (E'), loss modulus (E'') and

absolute value of modulus ($|E|$) of the PDMS nanocomposites were obtained by using dynamic mechanical analysis (DMA). Hardness of composites was evaluated by Shore-A hardness tests. The thermal properties of PDMSNC were investigated by thermogravimetric analysis (TGA). Surface properties were investigated by contact angle measurements and by using these data the surface free energy of the PDMS nanocomposites were calculated.

ÇAPRAZ BAĞLI POLİDİMETİL SİLOKSAN NANOKOMPOZİTLERİN SENTEZİ VE KARAKTERİZASYONU

ÖZET

Genel olarak kompozitler, iki veya daha fazla malzemenin kendi fiziksel ve kimyasal özelliklerini koruyarak oluşturdukları malzemelerdir. Kompozitteki kuvvetlendirici katkıların sürekli fazda homojen dağıtılması ile malzemenin yapısal özelliklerinde iyileştirme sağlanabilmektedir. Kompozit yapılar matris malzemesine göre metal, seramik, polimer kompozitler olarak sınıflandırılmaktadır. Klasik kompozitte katkılar matrise %10'dan fazla katılarak istenilen özellik sağlanmaya çalışılır. Nanokompozitlerde, klasik kompozitlere göre çok az miktarda katkı matris içerisinde homojen olarak dağıtılır. Kompozitler yapıları gereği anisotropi gösterirler. Ancak nanokompozitlerde katkının boyutundan dolayı bu durum çok belirgin değildir. Nanokompozitler, farklı kompozisyon veya yapılar içeren iki ya da daha fazla fazın ve katılardan en az birinin bir boyutunun nano ölçekli olduğu sistemlerdir. Bu malzemeler, yapısal birimlerinin küçük boyutta ve yüksek yüzey/hacim oranına sahip olmalarından dolayı mikro ölçekli geleneksel kompozitlerden farklı davranış sergilerler.

En çok kullanılan kompozit yapılardan biri polimer matris nanokompozitlerdir. Bunlar; polimerlerin, elyaf, pul, küre ve tanecik gibi belli geometriye sahip katkı maddeleri ile karışımlarından oluşmaktadır. Literatürde tabakalı silikat katkılar (killer) en çok çalışılan nanokatkılardır.

Polisiloksanlar, biyo malzemelerin elektrik izolasyonundan uzay araştırmalarına kadar çok çeşitli uygulama alanları için benzersiz özelliklere sahiptir. Poli (dimetil siloksan) (PDMS), polisiloksan grubunun en yaygın kullanılan üyesidir. Geniş molar hacim, kohezif enerji yoğunluğunun düşük olması ve esnekliğinin yüksek olması PDMS'nin önemli fiziksel özelliklerindedir. Bunlara ek olarak PDMS, görünür ve UV ışığına karşı saydam, ozon ve korona karşı çok dirençli, atomik oksijen ve hatta oksijen plazmalarına karşı karardır. Diğer üstün özellikleri ise film şekillendirme yeteneği, çeşitli gazlara karşı yüksek geçirgenliği, su sevmeyen (hidrofob) yapıda olması, serbest hareket yeteneği, yüzey aktivitesi, kimyasal ve fiziksel etkilere karşı etkisiz (inert) olmasıdır. Birçok üstün özelliğine karşın, PDMS kauçukların mekanik özelliklerini geliştirmek için molekül ağırlıklarının oldukça yüksek olması gerekmektedir.

Bu çalışmada tabakalı silikat olan Türk bentonitlerinin modifiye edilmesi ile oluşturulan çapraz bağlı poli (dimetil siloksan) nanokompozitlerinin (PDMSNK) hazırlanması amaçlanmıştır. Bu nanokompozitler alkil amonyum ve alkil fosfonyum tuzları kullanılarak modifiye edilen bentonitler ile değişen oranlarda (%3, 5 ve 10) in-situ polimerizasyon metodu ile hazırlanmıştır. Ayrıca yapılan testleri kıyaslama için organokil içermeyen çapraz bağlı PDMS hazırlanmıştır. Killerin modifikasyonu için heksadesiltrimetilamonyum klorür (HDTMAC), tribütilheksadesilfosfonyum bromür (TBHDPB) ve (4-karboksibutil)trifenilfosfonyum bromür (4CBTPPB) kullanılmıştır. Çapraz bağlanma dikünil peroksit ile yapılmış, hazırlanan çapraz

bağlı PDMS nanokompozit örnekleri ve organokiller; X-ışını kırınımı, evrensel test, Shore-A sertlik ve termogravimetrik analizler ile karakterize edilmiştir. Morfolojik araştırmalar X-ışını kırınımı (XRD) ve alan emisyon taramalı elektron mikroskopu (FE-SEM) ile yapıldı ve organokillerin ve PDMS nanokompozitlerin tabakalar arası uzaklıkları belirlendi.

Nanokatki bentonitin tabakalar arası uzaklığı (d_{001}) 13.86 Å'dir. Modifikasyonun kil tabakalarının arasını açtığı ve bu tabakalar arasına giren PDMS'in çapraz bağlanmasıyla "tabakaları tamamen dağılmış yapı" elde edildiği, çapraz bağlı PDMS nanokompozitlerinde XRD sonuçlarında d_{001} değerinin 44 Å'den büyük olduğu belirlenmiştir. Bu sonuç FE-SEM morfolojik ölçüm sonuçları ile uyumludur. Çünkü FE-SEM sonuçlarında killerin homojen dağılımı görülmüştür. Çapraz bağlı yapılarda, kilin malzemede dağılmasının çok iyi sağlanmasında pek çok parametre etkindir. Bilindiği gibi galeriler arası kürleşme hızı "kilin tabakaları tamamen dağıtılmış" yapıya ulaşmasında önemli bir faktördür ve galeriler arası kürleşme kürleşmenin başlangıcında gerçekleşir. Kilin bu yapıya ulaşması galeriler arası kürleşmenin hızının büyük olduğu durumlarda gerçekleşir. Kullandığımız sistemde de bu durum geçerli olmuştur.

TGA analiz sonuçlarına göre saf PDMS, PDMS-HDTMAC-B-5, PDMS-TBHDPB-B-5 ve PDMS-4CBTPPB-B-5'in bozunmaya başlama sıcaklıkları sırasıyla 491.8 °C, 499.1 °C, 493.3 °C ve 516.8 °C olarak bulunmuştur. Aynı zamanda yapısındaki fenil gruplarından dolayı PDMS-4CBTPPB-B nanokompozitin bozunma sıcaklığı PDMS-HDTMAC-B ve PDMS-TBHDPB-B nanokompozitlerine kıyasla daha çok artmıştır. Bozunma sona erdikten sonra, saf PDMS, PDMS-HDTMAC-B-5, PDMS-TBHDPB-B-5 ve PDMS-4CBTPPB-B-5'in ortamda kalan karbon yüzdeleri sırasıyla %24, %27.5, %27 ve %27 olup, bozunmanın bittiği sıcaklıkları ise 598, 584, 587 ve 596 °C'dir

Evrensel test cihazından alınan gerilim-gerinim sonuçlarından, elastik modülü ve kopma uzaması ile çekme mukavemeti değerleri hesaplanmıştır. Çekme test sonuçlarına göre, %3 organokil içerikli nanokompozitlerin E-modülü değerlerinin saf PDMS'e göre fazla değişiklik göstermiyorken, %5 ve %10 oranında organokil içeren nanokompozitlerin E-modül sonuçları tüm modifiye bentonit içeren nanokompozitler için artışa neden olmuşlardır. Bunun yanında HDTMAC ile modifiye edilen bentonit ile hazırlanan PDMS nanokompozitlerin, TBHDPC VE 4CBTPPB ile modifiye edilmiş bentonitlerle hazırlanan PDMS nanokompozitlere kıyasla daha iyi özellikler sergilediği gözlenmiştir.

Depo modülü (E'), kayıp modülü (E'') ve modülün mutlak değeri ($|E|$) dinamik mekanik analiz (DMA) cihazı kullanılarak elde edilmiştir. Düşük frekanslarda E' değeri düşüktür. Çünkü en fazla deformasyon malzemenin viskoz kısmından gelir. Yüksek frekanslarda modülün mutlak değeri (E')'a eşittir. Çünkü yüksek frekanslarda, bir salınım devri için geçen zaman boyunca viskoelastik malzemenin viskoz kısmında kayda değer bir akış için yeterli bir zaman olmaz. Hareket, malzemenin elastik kısmının gerilimi sonucu oluşur. Bu nedenle dinamik modül (E'), malzemenin elastik kısmının modülüne eşit olur. DMA sonuçları göre PDMSNC örnekleri viskoelastik malzeme davranışını desteklemektedir.

Çapraz bağlı PDMS nanokompozitlerin sertlikleri Shore-A sertlik ölçümleri ile belirlendi. Sertlik ölçüm sonuçları kil yüzdesindeki artışla çok belirgin bir artış göstermediğinden, nanokatksız PDMS'e göre, kilin sertliğe bir etki yapmadığı ifade edilebilir.

Temas açısı ölçümleri ile yüzey özellikleri incelenmiş ve bu veriler kullanılarak yüzey serbest enerjileri hesaplanmıştır. Çapraz bağlı PDMS nanokompozitlerin temas açılarını ölçmek ve yüzey davranışlarını belirlemek için deiyonize su, diiyodometan ve etilen glikol kullanılmıştır. Temas açısı test sonuçlarına göre, HDTMAC ve 4CBTPPB ile modifiye edilmiş bentonit ile hazırlanan PDMS nanokompozitlerin su temas açıları saf PDMS'e göre değişiklik göstermezken, TBHDPB ile modifiye edilmiş bentonit ile hazırlanan PDMS nanokompozitlerin su temas açısı değerleri saf PDMS'e göre 104°'den 81.1°'e düşmüştür. Bu sonuçlara göre TBHDPB ile modifiye edilmiş bentonit ile hazırlanan PDMS nanokompozitlerde hidrofilik yapı olduğu gözlenmiştir.

1. INTRODUCTION

Nanocomposites constitute one of the most advanced areas of nanotechnology. Especially, organoclays based nanocomposites have exhibited improved properties compared to conventional polymer composites containing traditional fillers [19].

Polymer-clay nanocomposites are particulate-filled composites in which the reinforcement material is in the form of sheets with thickness of one to few nanometers and length of hundreds to thousands of nanometers. Layered silicates which is a structural group of 2:1 phyllosilicates and an undergroup of smectites can be used for the synthesis of polymer-clay nanocomposites. Pristine layered silicates usually contain hydrated sodium or potassium ions. Ion-exchange reactions with cationic surfactants, including primary, tertiary and quaternary ammonium/phosphonium ions, render the normally hydrophilic silicate surface organophilic, which makes intercalation of many engineering polymers possible and improve the wetting characteristics with the polymer in which the surface energy of clay decreases and the basal spacing expands. The organoclays are abundant, inexpensive, environmentally friendly and above all essential to develop polymer nanocomposites. All of these properties attracted researchers to surface modification of clays which creates new materials to be used in a wide spectrum of new applications [36].

Elastomeric nanocomposites represent an interesting subgroup. Elastomeric silicones are widely used where elastomers come in contact with food and pharmaceuticals. Different curing methods can be applied for crosslinking this elastomer. Silicone elastomers are obtained by the of functionalized poly (dimethyl siloxane).

Siloxanes, the building blocks for silicone products, are widely used chemicals in many versatile applications. The siloxanes are characterised by a high stability, physiologically inertness, good release and lubricating properties [35].

Siloxanes are chemical compounds with a backbone of alternating silicon (Si) and oxygen (O) atoms, in which each silicon atom are bonded to one or several organic

groups. Siloxanes are building blocks for silicone products or they constitute a part of other products, such as cosmetics or paint. In colloquial language the term silicones is often used synonymously with siloxanes. The properties of the siloxanes and the silicone products depend on the length of the Si-O backbone, the chemical groups attached to this backbone and the presence of any cross-links between the backbones. Silicone products can be subgrouped into three, such as silicone fluids, elastomers and resins. Silicone fluids are used for a wide range of applications. Silicone elastomers are mainly used for sealants and rubbers, and resins are mainly used for paints. The most common siloxanes are poly (dimethylsiloxane) (PDMS) with different modifications [30].

In this study, the cross-linked PDMS nanocomposites were prepared by in-situ polymerization method by using alkyl ammonium or alkyl phosphonium modified bentonites at varying compositions. The cross-linked PDMS without organoclay was also prepared for the comparison purposes. The modifiers were hexadecyltrimethylammonium chloride and (4-carboxybutyl) triphenylphosphonium bromide. The pure cross-linked PDMS rubber and its nanocomposites were characterized by morphological, thermal and mechanical analysis. Structural analysis of the prepared organoclays and PDMS nanocomposites were determined by Fourier transform infrared spectroscopy (FTIR). The morphological investigations were performed by x-ray diffraction (XRD) and scanning electron microscopy (SEM) to obtain the interlayer distance of PDMSNCs. Elastic modulus, tensile strength and elongation at break values were determined by tensile tests. Storage modulus (E'), loss modulus (E'') and absolute value of modulus ($|E|$) of the PDMS nanocomposites were obtained by using dynamic mechanical analysis (DMA). Hardness of composites was evaluated by Shore-A hardness tests. The thermal properties of PDMSNC were investigated by thermogravimetric analysis (TGA). Surface properties were investigated by contact angle measurements and by using these data the surface free energy of the PDMS nanocomposites were calculated.

2. THEORETICAL PART

2.1 Composite Materials

A composite material is defined such that combination of two or more materials in which the constituents retain their identities. Those constituents do not dissolve or merge completely in each other; however, they can be physically identified and act together [1]. For superior properties, such as lighter weight and higher strength, compared to those of the individual components, they are dispersed in a controlled way, which means relative amounts, the geometry of the dispersed phase, particle size, distribution and orientation affect [2].

Composites usually consist of two different phases; the first one is the continuous phase which is called the matrix. This phase acts as a binder that holds the components together and it is the main load-bearing constituent, so that it governs the mechanical properties of the materials. The second one is the reinforcement that is dispersed in the continuous phase. The main advantage of this phase is its strength, stiffness and hardness relative to the matrix phase [3]. Reinforcement phase can be in the form of either continuous (long fibers, sheets) or discontinuous (particles, short fibers, etc.). Particle-reinforced composite group includes single layer and multi-layer composites that are composed of laminates (sheet constructions in a specified sequence), hybrids (construction with mixed fibers in ply or layer by layer) and sandwich panels (structural composites with two outer sheets separated by a layer of less dense material) [4].

Another parameter that affects the properties of composites is the existence of the matrix and reinforcement interface, i.e. interphase. Failure mechanism, fracture toughness and overall stress-strain behavior of the material are generally determined by this separate phase [5]. Wettability, surface roughness and bonding are the factors that the interphase depends on. These three factors are mainly related to one another. For instance, surface roughness has a prominent effect on wettability

since it can reduce the bonded area and lead to void formation or stress concentrations [4].

There are different types of interfacial bonding mechanisms at the interphase. Mechanical bonding is one of these interfacial bonding types, it is efficient in load transfer when the force is applied parallel to the interface. However, pure mechanical bondings such as molecular chain entanglement and inter-diffusion at the interface have low strength compared to chemical bonding, which includes bonding by direct reactions, coupling agents. In addition, physical bonding is another important type of bonding mechanism. Physical bonding involves weak, secondary, van der Waals forces, dipolar interactions and hydrogen bonding; like mechanical bonding it is not enough for most of the cases owing to its effectiveness over small distances [6].

Composite structures can be classified according to the matrix material that they are made up of. The matrix can be metal, ceramic, polymer, etc. In composites with metal matrix, reinforcement improves specific stiffness, strength, abrasion resistance, creep resistance, thermal conductivity and dimensional stability. Also, their resistance to degradation, non-flammability and operating temperatures can be enhanced by organic fluids. For ceramic matrix composites, fibers are incorporated into them to preserve the high processing temperature and they have inherent resilience to oxidation and deterioration [2].

2.1.1 Polymer matrix composites

One of the most widely used types of composite structure is polymer matrix composites. They are mixtures of polymers with inorganic and organic additives having certain geometries, such as fibers, flakes, spheres and particulates. Polymers have many advantages over other types of materials, since processing polymers does not require high pressure and high temperatures, and the processing cost is low. Also, they have low density and have many useful characteristics, such as tensile strength, modulus, elongation and impact strength [7].

Polymers can be categorized into two main groups: thermoplastics and thermosets. Thermoplastics are linear or branched structure materials with no chemical linking between them. By the application of heat and pressure, weak secondary forces such as van der Waals and hydrogen forces are broken temporarily and material takes a new shape. Upon cooling, the secondary forces are restored resulting in a new solid

shape. On the other hand, thermoset polymers are crosslinked networks. When they are heated, they undergo curing reactions, so they could be made to flow under stress only once. If further heating is applied degradation occurs and no softening or flow can be seen [8]. In uncured state, thermoset polymers have low viscosities compared to thermoplastic materials; this facilitates the wetting out of the reinforcement. However, their hard processing and long production rates make them less preferable compared to thermoplastics.

2.2 Nanocomposites

Nanocomposites are a combination of two or more phases containing different compositions or structures, where at least one of the phases is in the nanoscale regime. These materials exhibit behavior different from conventional composite materials with microscale structure, due to the small size of the structural unit and the high surface-to-volume ratio [9]. Nanocomposites are classified into three main classes, depending on the shape of the nanofiller, i.e., the number of dimensions of the dispersed particles in the nanometer range.

(a) *Nanoparticulate composites* composed of embedded isodimensional particles with three dimensions in the order of nanometers, such as spherical silica nanoparticles, semiconductor nanoclusters [10,11].

(b) *Nanofilamentary composites* composed of a matrix with embedded (generally aligned) nanoscale diameter filaments. In this type, two dimensions are in the nanometer scale and the third one is larger, forming an elongated structure such as, carbon nanotubes or cellulose whiskers which are extensively studied as reinforcing nanofillers yielding materials with exceptional properties [10,11].

(c) *Nanolayered composites* composed of alternating layers or sheets in which only one dimension is in the nanometer range. In this case, the filler is in the form of sheets (i.e., silicates) one to a few nanometers thick and hundreds to thousands nanometers long. Polymer-layered crystal nanocomposites belong to this group. These materials are almost exclusively obtained by the intercalation of the polymer (or a monomer subsequently polymerized) inside the galleries of layered host crystals [10,11]. Nanolayered composites based on layered silicates have been more widely investigated; probably because of the abundance of the starting clay materials and the variety of advantages they offer [10].

2.2.1 Polymer-layered silicate nanocomposites

As mentioned previously, depending on the nature of the components and processing conditions, layered silicates filled into a polymer matrix, produce either conventional composite or nanocomposite [12].

2.2.2 Structure of layered silicates

Fillers are added into polymer matrix to enhance physical properties such as mechanical, thermal, flame retardancy, processing characteristics, and barrier properties or to lower the cost. In order to improve the mechanical properties of polymer matrix composites, high aspect ratio (glass fibers, mica, clay minerals, and carbon nanotubes) and low aspect ratio (talc, kaolin, CaCO₃, glass spheres, and wood flour) fillers can be used.

Clay minerals are hydrous aluminum silicates and are generally classified as phyllosilicates, or layered silicates. Layered silicates that are used in the preparation of polymer-layered silicate nanocomposites belong to the 2:1 phyllosilicates family and they are among the large number of inorganic layered materials that have the capability of intercalation [13]. Their crystal lattices are generated by a combination of tetrahedral and octahedral sheets. In order to form 2:1 layered silicates, a natural stacking of those tetrahedral and octahedral sheets occurs in the specific ratios and modes. Silica is the main component of a tetrahedral sheet, while octahedral sheet comprises diverse elements such as Al, Mg, and Fe. Those sheets are arranged as 1 nm thin layers, with an octahedral sheet sandwiched between two tetrahedral silica sheets. These layers organize themselves to form stacks with a regular van der Waals gap between them, which is called the interlayer, gallery or basal spacing. This distance between the sheets of silicate layers can be determined by X-Ray Diffraction patterns.

The phyllosilicate 2:1 layer clays include mica, smectite, vermiculite, and chlorite. Smectite group can be further divided into montmorillonite (MMT), saponite and hectorite species [14]. Their chemical formulas are shown in Table 2.2 and chemical structures are given in Figure 2.1 [15].

Table 2.1 : Chemical formulas of commonly used smectite type layered silicates

Layered Silicate	General Formula*
Montmorillonite	$M_x(Al_{4-x}Mg_x)Si_8O_{20}(OH)_4$
Saponite	$M_xMg_6(Si_8-xAl_x)O_{20}(OH)_4$
Hectorite	$M_x(Mg_6-xLi_x)Si_8O_{20}(OH)_4$

*M = monovalent cation; x = degree of isomorphous substitution.

Montmorillonites have 2:1 type layered structure. Crystal like structure of the montmorillonite occurs from, silicon-oxygen (Si-O) tetrahedral layer with (Al-OOH) octahedral layer which is between two Si-O layers. Silicon atoms are bonded with 4 oxygen atoms in (Si-O) layers. Oxygen atoms are placed regularly as one in centre of silicon atom and the other 4 atoms are on the corners of the tetrahedron (Figure 2.1). Layers are divided between every third neighbour tetrahedral layer structure from 4 oxygen atoms of tetrahedron layer. All of the fourth oxygen atom of the tetrahedron has condition as oriented to lower side of structure which can be seen in Figure 2.1 and they are at the same plane with the -OH groups of alumina octahedral layers [16,17].

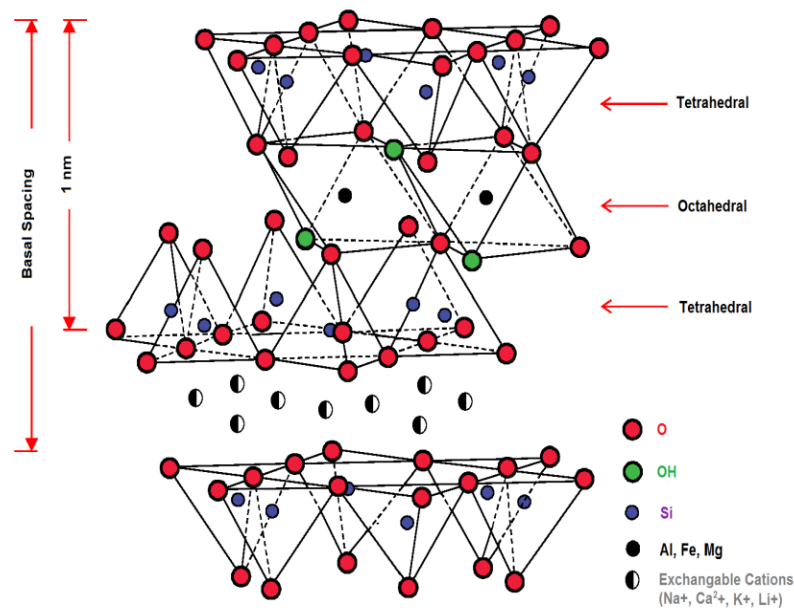


Figure 2.1 : Structure of 2:1 phyllosilicates [16,17].

2.2.2.1 Bentonite

Bentonite clays, currently in use in over a hundred areas, are among the most important industrial raw materials. Principal clay minerals of bentonites are smectites

such as montmorillonite, beidellite, saponite, nontronite, hectorite, and laponite. Bentonites are predominantly consists of montmorillonite rather than othersmectites.

A smectite is a 2:1 layer clay mineral and has two silicatetrahedral (T) sheets bonded to a central alumina octahedral (O) sheet. Smectites are described either dioctahedral ortrioctahedral depending upon whether the octahedral cations are predominantly trivalent or divalent, respectively [18].

Main uses for bentonite are in foundry sands; drilling muds, iron ore pelletizing, absorbents, as a variety of composite liners, food additive for poultry and domestic animals, in filtration, foods, cosmetics and pharmaceuticals. Bentonite is part of the most adsorbent, bleaching and catalyst clays. About 6 million tons of bentonite is produced annually [19].

2.2.2.2 Organic modification of bentonite

There are many mechanisms for modification of clay surfaces such as adsorption, ion exchange with inorganic and organic cations, binding of inorganic and organic anions, grafting of organic compounds, reaction with acids, pillaring by different types of poly (hydroxo metal) cations, intraparticle and interparticle polymerization, dehydroxylation and calcination, delamination and reaggregation of smectites, lyophilisation, ultrasound, and plasma. Modified clays are also used in other applications such as adsorbents of organic pollutants in soil, water and air; rheology control agents, paints, cosmetics, refractory varnish, thixotropic fluids, etc. [20].

The hydrophilic structure of MMT and other layered silicates present a problem of incompatibility to mix and to disperse in the organic hydrophobic polymers. The electrostatic forces holding the clay platelets tightly together cause another problem. In order to overcome these problems, the layered silicates should be organically modified. One way of modifying clay surface is to make it more compatible with a polymer through ion exchange reactions. Since the inorganic cations on the clay surface are not strongly bound, they can be replaced by other organic cations, which are tailored to the polymer in which the clay would be incorporated. For example one side of the molecule can have a quaternary ammonium ion with the other side of the molecule having a long chain alcohol group [21]. This process of ion exchange (Figure 2.2) would help render the hydrophilic surface hydrophobic (polymer compatible) by matching the clay surface polarity with the polarity of the polymer

[22] and also to separate the clay platelets so that they can be more easily intercalated and then subsequently exfoliated into the polymer [21]. In addition, the organic cations may provide various functional groups that can react with the polymer chain to increase adhesion between the inorganic filler and the organic polymer matrix [23].

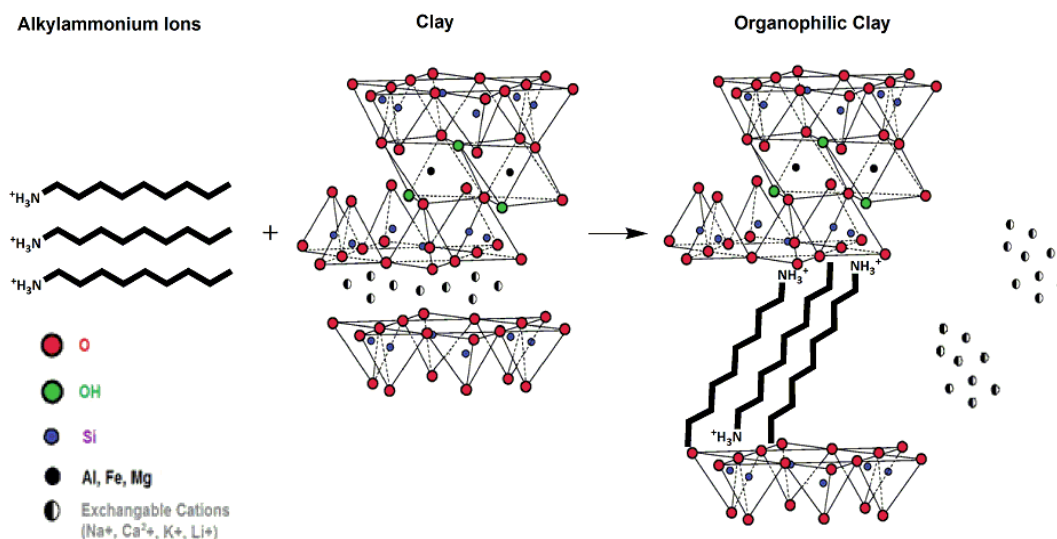


Figure 2.2 : Cation exchange process between alkylammonium ions and exchangeable cations of layered silicate structure and dynamics of polymer-layered silicate nanocomposites [23,24].

Depending on the charge density of the clay and the onium ion surfactant, different arrangements of the onium ions as monolayer, lateral bilayer, pseudo-trimolecular layer, and inclined paraffin structure are possible (Figure 2.3) [22].

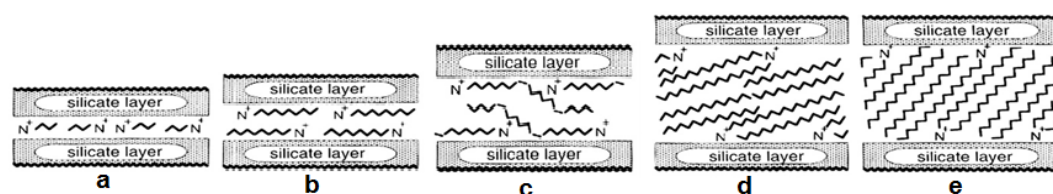


Figure 2.3 : Orientations of alkylammonium ions in the galleries of layered silicates: (a) monolayer, (b) bilayers, (c) pseudo-trimolecular layers, and (d, e) paraffin-type arrangements of alkylammonium ions with different tilting angles of the alkyl chains [22].

Figure 2.3 shows the types of nanocomposite structures. If the polymer cannot intercalate into the galleries of clay minerals, conventional microcomposite is obtained with properties similar to that of polymer composites reinforced by microparticles. Intercalated nanocomposite is produced when a monolayer of

extended polymer chains is inserted into the gallery of clay minerals resulting in a well ordered multilayer morphology, stacking alternately polymer layers and clay platelets and a repeating distance of a few nanometers. Exfoliated or delaminated nanocomposite forms when the clay platelets are completely and uniformly dispersed in a continuous polymer matrix. However, it should be noted that in most cases the cluster nanocomposite is common in polymer nanocomposites [12].

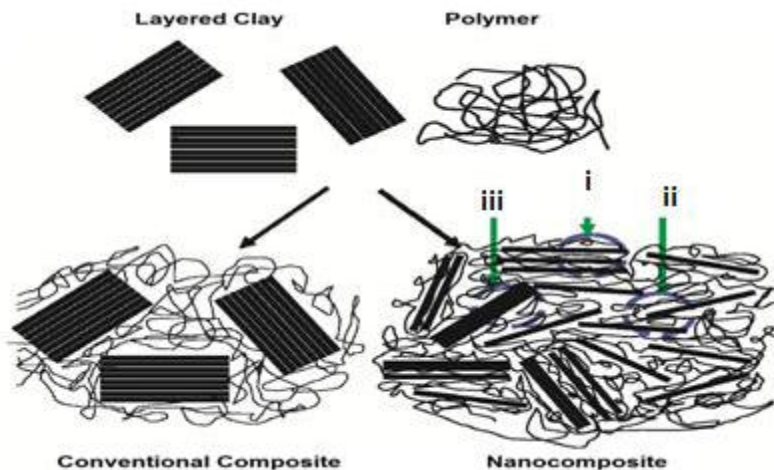


Figure 2.4 : Schemes of polymer/clay composites, including conventional composite and nanocomposite with intercalated (i), exfoliated (ii) or cluster (iii) structure [12].

2.2.3 Nanocomposite preparation techniques

Polymer-layered silicate nanocomposites can be prepared by various methods including; in-situ polymerization, solution intercalation, melt intercalation and sol gel.

2.2.3.1 In-Situ polymerization method

In in-situ polymerization method, a liquid monomer (or a monomer solution) is inserted between the galleries of the layered silicates and then polymerized within the gallery via an initiator such as, heat, radiation, pre-intercalated initiators or catalysts [12]. The swelling step depends on the polarity of the monomer molecules, the surface treatment of the organoclay, and the swelling temperature. The high surface energy of the clay attracts polar monomer molecules so that they diffuse between the clay layers and intercalate them. Then, polymerization reaction starts by the attraction between the monomer and the curing agent. Finally, the delamination of organic molecules within the clay layers occurs (Figure 2.5). The polymerization

initiator for thermosets, such as epoxies or unsaturated polyesters, can be a curing agent or peroxide, respectively. For thermoplastics, the polymerization can be initiated either by the addition of a curing agent or by an increase of temperature. In situ polymerization is the first method used to synthesize polymer-layered silicate nanocomposites based on polyamide 6 [25].

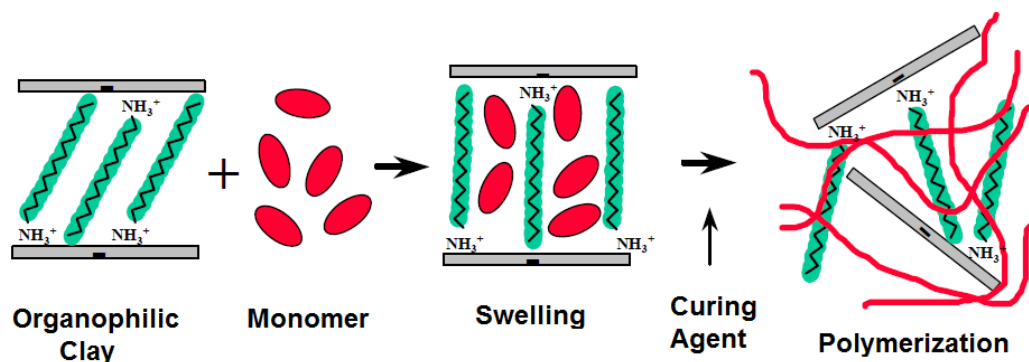


Figure 2.5 : In-Situ polymerization method [25]

2.2.3.2 Solution intercalation method

In solution method, layered clays are separated into single platelets due to the weak van der Waals forces that hold the clay platelets together using a solvent in which the polymer is soluble. Then, the polymer, dissolved in the solvent, is added to the clay suspension and intercalates between the clay layers. The solvent is finally removed from the clay-polymer complex through evaporation (Figure 2.6). [12, 25].

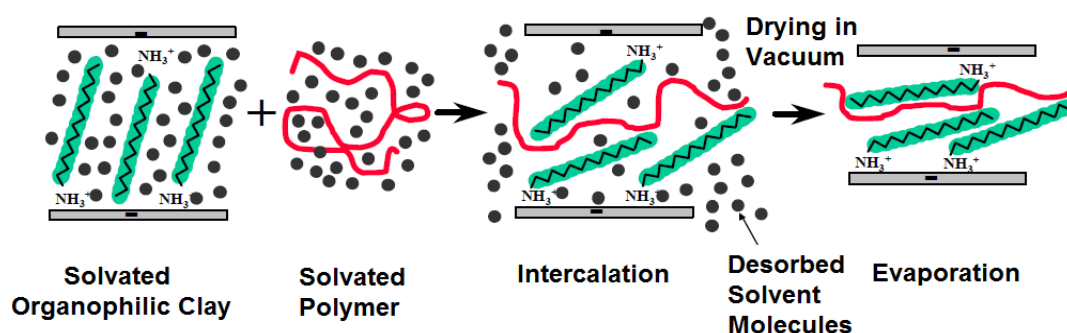


Figure 2.6 : Solution intercalation method [25]

The entropy, which is gained by desertion of the solvent molecules, is the drivingforce of this method. The decrease in conformational entropy of the intercalatedpolymer chains is compensated with the entropy gained by desorption of thesolvent molecules. For that reason, large number of solvent molecules must be desorbed from the clay to accommodate the incoming polymer chains. This method

is suitable for the polymers with little or no polarity. However, the use of large amount of inorganic solvents that is environmentally unfriendly and economically prohibitive is one of the major drawbacks [43].

2.2.3.3 Melt mixing method

Melt mixing process involves heating a polymer and layered silicate mixture above the glass transition temperature under static or flow conditions in the absence of solvent. The polymer chains spread from the molten mass and invade the silicate galleries, to form either intercalated or delaminated hybrids according to the degree of penetration (Figure 2.7). Polymer compatible modified layered silicates are usually employed to promote intercalation. A gain in entropy, due to the greater conformational energy of the aliphatic chains of the alkylammonium cations due to the increase in the size of the galleries caused by insertion of the polymer, is suggested to be the driving force for a spontaneous melt intercalation process [26, 27].

The melt mixing process has become popular because of its great potential for application in industry. Indeed, polymer-clay nanocomposites have been successfully produced by extrusion of a wide range of thermoplastics, from strongly polar polyamide, to weakly polar PET to non-polar polystyrene. Polyolefins, which represent the biggest volume of polymers produced, have so far only been successfully intercalated to a limited extent [25]. Direct polymer melt intercalation is also known as the most attractive way because of its low cost, high productivity and compatibility with current polymer processing techniques [28].

In addition to absence of solvent in melt intercalation process, it differs from other preparation methods in the strong shear forces acting on the system, which affect the dispersion of clay platelets. Besides, matrix viscosity and the mean residence time also affect the degree of the dispersion [29].

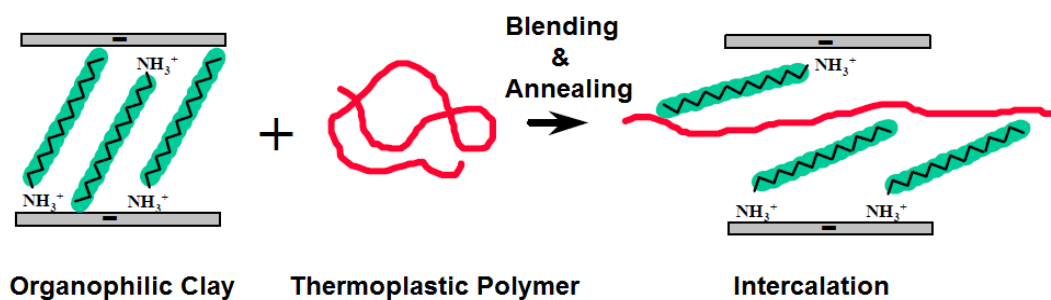


Figure 2.7 : Melt mixing method [25]

2.3 Polysiloxanes

Polysiloxanes, which are usually known as “silicones” or “silicon elastomers”, have received wide spread attention as specialty polymers since their commercial introduction in the 1940’s and are by far the most important of the inorganic backbone polymers. Special interest in these systems has developed as a result of their unique properties which fulfill a wide range of needs for very diversified applications ranging from electrical insulation to biomaterials and to space research. Thermodynamic calculations and spectroscopic studies have shown that in poly (dimethyl siloxanes), $[(CH_3)_2SiO]_n$, the methyl groups rotate with unusual ease around the (Si-O) bonds. A large molar volume ($75.5 \text{ cm}^3/\text{mole}$) and a low cohesive energy density (intermolecular forces) of poly (dimethyl siloxanes) (PDMS) are consequences of the ease of rotation of the methyl groups. Low intermolecular forces and the flexibility are also responsible for many unique properties of the PDMSs such as extremely low glass transition temperature ($T_g = -123 \text{ }^\circ\text{C}$), low surface tension and surface energy, low solubility parameter and low dielectric constant. In addition, poly (dimethyl siloxanes) are transparent to visible and UV light, very resistant to ozone and corona discharge, stable against atomic oxygen and even oxygen plasmas. Moreover, these properties show only a very small variation over a wide temperature range. Other outstanding properties include film forming ability, high permeability to various gases, hydrophobic behaviour, release action, surface activity and chemical and physiological inertness.

Despite their many outstanding properties, PDMS rubbers require extremely high molecular weights to develop useful mechanical properties.

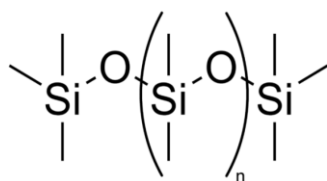


Figure 2.8 : Chemical backbone structure of PDMS

Even at a molecular weight of 500,000 g/mole they exhibit cold flow and very weak rubbery properties. Therefore, PDMS must generally be chemically crosslinked in order to be used in an elastomer. However, unfilled PDMS vulcanizates still have very low tensile and tear strengths and elongations. Polysiloxanes are not compatible with the numerous organic polymers due to their low solubility-parameter ($7.5 \text{ (Cal cm}^{-3})^{1/2}$). In addition, they have high gas permeability, chemically and physically inert and hydrophobic properties [30].

Table 2.2 : Properties of PDMS [31]

Property	Value
Mass density	0.97 kg/m ³
Young's modulus	360-870 KPa
Poisson ratio	0.5
Tensile or fracture strength	2.24 MPa
Specific heat	1.46 kJ/kg K
Thermal conductivity	0.15 W/m K
Dielectric constant	2.3-2.8
Index of refraction	1.4
Electrical conductivity	$4 \times 10^{13} \Omega\text{m}$
Magnetic permeability	$0.6 \times 10^6 \text{ cm}^3/\text{g}$
Adhesion to silicon dioxide	Excellent
Biocompatibility	Nonirritating to skin, no adverse effect on rabbits and mice, only mild inflammatory reaction when implanted
Hydrophobicity	Highly hydrophobic, contact angle 90-120°
Melting Point	-49.9–40°C

The alternating silicon and oxygen atoms form a backbone structure to which different side chains are linked. The side chains may form cross links which influence the properties of the polymer. The silicon and oxygen atoms may be linked into cyclic or linear structures, and we distinguish between *linear siloxanes* and *cyclic siloxanes*.

2.3.1 Linear siloxanes

Linear polysiloxanes are characterised by the functional side chains attached to the Si-O backbone and the endgroups terminating the structure (illustrated by R5). The side groups may be the same group or several different side groups may be attached (illustrated by R1-R4).

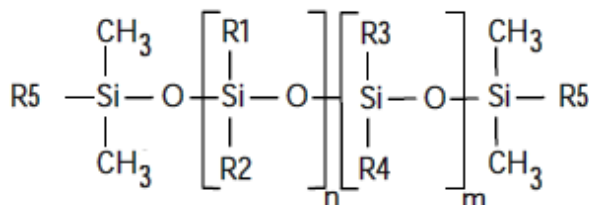


Figure 2.9 : Linear siloxane structure

Linear poly (dimethyl siloxanes) are the most important industrial polysiloxanes. In their most simple form they consist of methyl side-chains and methyl terminal groups, poly (dimethyl siloxane) (PDMS). The shorter linear polysiloxanes are, like some of the cyclic siloxanes mentioned below, volatile. The shortest, hexamethyldisiloxane, is volatile with a boiling point of 100°C, and is used in cosmetics among other applications.

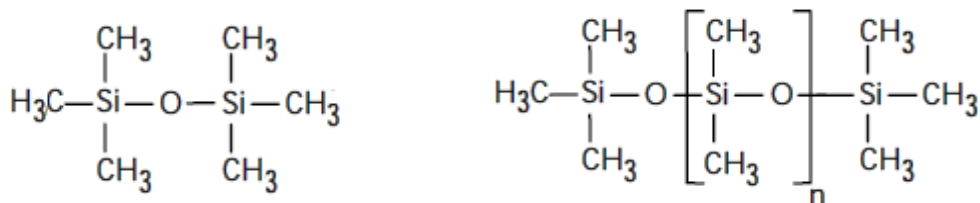


Figure 2.10 : Hexamethyl disiloxane **Figure 2.11 :** Poly (dimethyl siloxane) (PDMS)

The end groups determine the use of the polymer. Typical end groups are methyl, hydroxyl, vinyl or hydrogen. For example; poly (dimethyl siloxanes) are typically silicone fluids, whereas vinyl- and hydroxyterminated polysiloxanes find major application in silicone elastomers. Major functional side groups are vinyl, aminopropyl, polyether, phenyl, trifluoropropyl, phenylethyl tetrachlorophenyl, and alkylene oxide. Hundreds of different compounds exist [40].

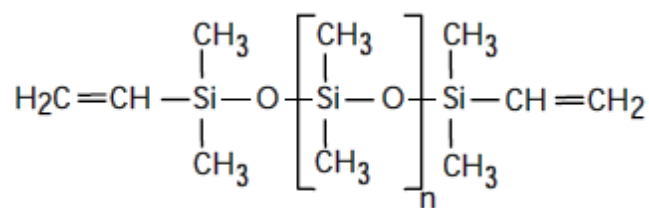


Figure 2.12 : Vinyl terminated poly (dimethyl siloxane)

2.3.2 Cyclic siloxanes

Cyclic siloxanes are partly used as intermediates for the production of higher molecular weight linear siloxanes, partly used directly as fluids. In the cyclic siloxanes the Si-O backbone forms a cyclic structure with two substituents attached to each silicium atom. The main compounds, octamethylcyclotetrasiloxane and decamethyl cyclopentasiloxane are used for a large number of applications. The two compounds are volatile, with boiling points of 176°C and 210°C respectively [40].

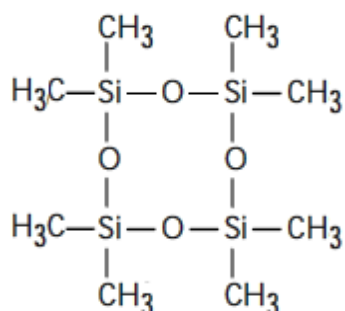


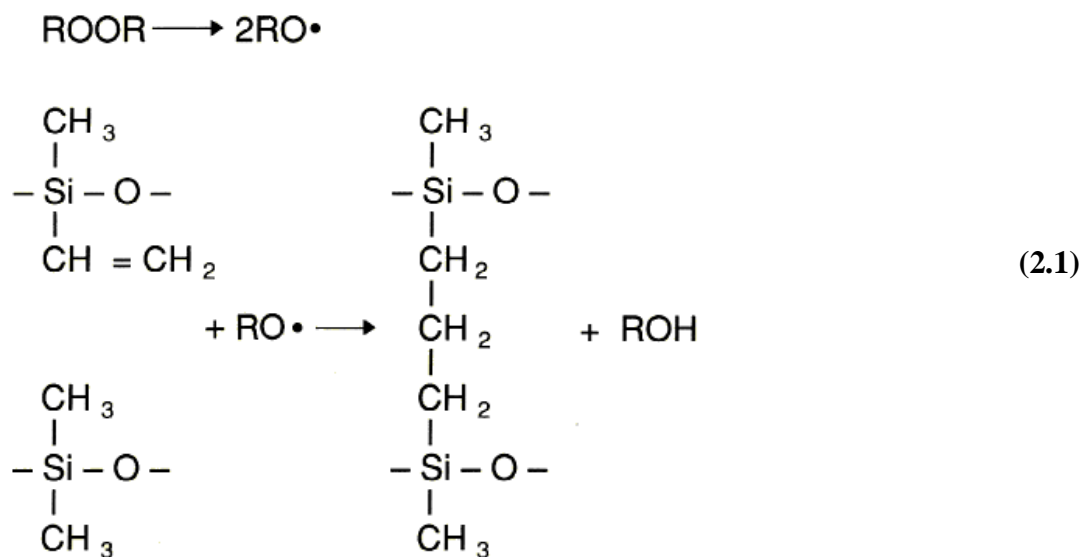
Figure 2.13 : Octamethyl cyclotetrasiloxane

2.4 Cross-linking of Poly (dimethyl siloxane) (PDMS)

Silicone fluids can be used "as supplied." In other words, their properties are fully developed. Silicone gels, elastomers, and resins, however, may need to be crosslinked (or cured) to achieve their final properties. This requires the presence of a crosslinker, a silicone molecule with multiple functional sites that can react or link with another silicone polymer. Under the proper conditions (i.e. heat, humidity, or ultraviolet light) – and in the presence of the crosslinker and a catalyst – the individual polymer chains will link together to form a more complex material. Depending on the base polymer, the crosslink density, and the presence of any reinforcing fillers, this material can range from a rigid film to a flexible rubber or a spongy. This is achieved according to one of the following reactions:

2.4.1 Cross-linking with radicals

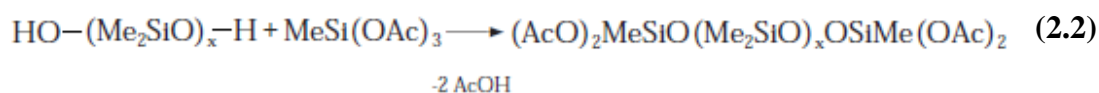
Efficient cross-linking with radicals is achieved only when some vinyl groups are present on the polymer chains. The following mechanism has been proposed for the cross-linking made by radicals generated from an organic peroxide shown in Equation 2.1:



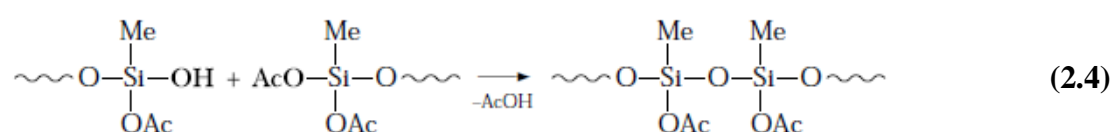
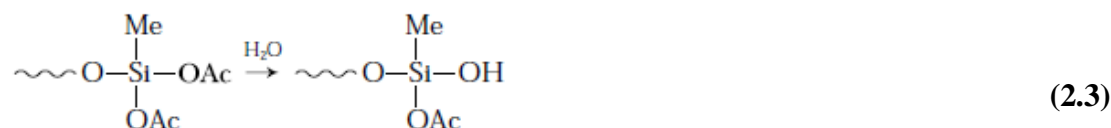
This reaction is used for high-consistency silicone rubbers (HCR) like the ones used in extrusion or injection molding and which are cross-linked at elevated temperatures. The peroxide is added before use. During cure, some precautions are needed to avoid the formation of voids by the peroxide's volatile residues. Postcure may also be necessary to remove these volatiles, which can act as depolymerization catalysts at high temperatures.

2.4.2 Cross-linking by condensation

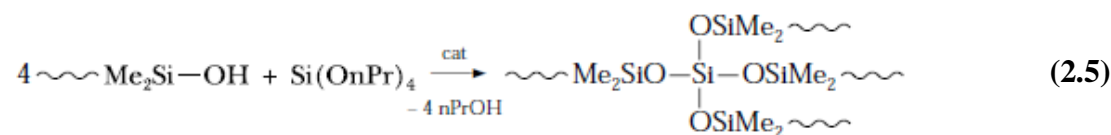
This method is used in sealants such as the ones available in do-it-yourself shops. These products are ready-to-use and require no mixing. Cross-linking starts when the product is squeezed from the cartridge and comes into contact with moisture. They are formulated from a reactive polymer prepared from a hydroxy endblocked poly(dimethyl siloxane) and a large excess of methyltriacetoxysilane:



As a large excess of silane is used, the probability of two different chains reacting with the same silane molecule is remote and all the chains are endblocked with 2OAc functions. The resulting product is still liquid and can be stored in sealed cartridges. Upon opening and contact with the moisture of the air, the acetoxy groups are hydrolyzed to give silanols that allow further condensation to occur:



In this way, two chains have been linked, and the reaction will proceed further from the remaining acetoxy groups. An organometallic tin catalyst is normally used. This cross-linking requires that moisture diffuses within the product and the cure will proceed from the outside surface toward the inside. These sealants are called one-part RTV (room temperature vulcanization) sealants, but they actually require moisture as a second component. Acetic acid is released as a by-product of the reaction and corrosion problems are possible on substrates such as concrete, with the formation of a water-soluble salt at the interface (and loss of adhesion at the first rain). To overcome this, other systems have been developed, including one-part sealants releasing less corrosive or noncorrosive byproducts. Condensation cure is also used in two-part systems where cross-linking starts upon mixing the two components, e.g., a hydroxy endblocked polymer and an alkoxy silane such as tetran-propoxysilane:



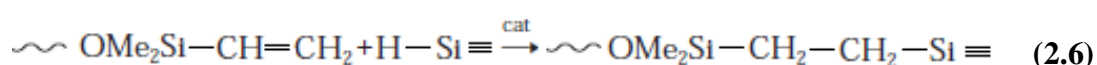
Here, no atmospheric moisture is needed. Usually an organotin salt is used as catalyst; however, to do so limits the stability of the resulting elastomer at high

temperatures. Alcohol is released as a by-product of the cure, leading to a slight shrinkage upon cure.

This precludes the fabrication of very precise objects (0.5 to 1 % linear shrinkage).

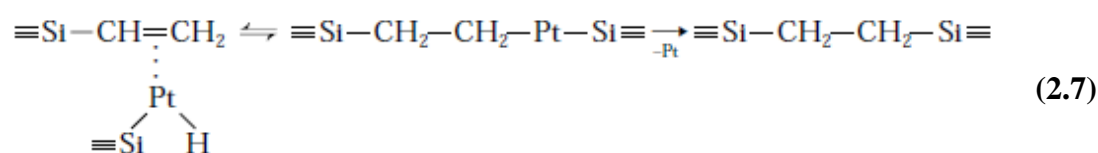
2.4.3 Cross-linking by addition

The above shrinkage problem can be eliminated when using an addition reaction to achieve cross-linking. Here, cross-linking is achieved using vinyl end blocked polymers and reacting them with Si-H groups carried by functional oligomers such as those described above. A few polymers can be bonded to this functional oligomer, as follows:



where \equiv represents the remaining valences of the Si

The addition occurs mainly on the terminal carbon and is catalyzed by Pt or Rh metal complexes, preferably organometallic compounds to enhance their compatibility. The following mechanism has been proposed (oxidative addition of the $\equiv\text{SiH}$ on the Pt, H transfer on the double bond, and reductive elimination of the product):



where to simplify, other Pt ligands and other Si substituents are omitted.

There is no by-product with this reaction. Molded pieces made with a product using this cure mechanism are very accurate (no shrinkage). However, handling these two-part products (polymer and Pt catalyst in one component, Si-H oligomer in the other) require some precautions. The Pt in the complex is easily bonded to electron-donating substances such as amine or organosulphur compounds to form stable complexes with these poisons, rendering the catalyst inactive (inhibition) [32].

2.5 Literature Overview of Siloxane Nanocomposites

In the study made by Giannelis and Burnside, the nanocomposites were synthesized by sonicating at room temperature with silanol-terminated poly (dimethylsiloxane) and commercial organosilicate. Organosilicate was prepared with dimethyl ditallow ammonium bromide and sodium montmorillonite. Cross-linking was accomplished by tetraethyl orthosilicate and curing was made at room temperature. Silicate delamination was optimized by adding water during the initial sonication. The superior mechanical properties of siloxanes at elevated temperatures usually justify their increased cost over conventional elastomer. Thus, thermal stability especially at elevated temperatures is an important characteristic in these materials. The nanocomposite shows delayed decomposition compared to the unfilled polymer. Additionally, the nanocomposites exhibit a substantial decrease in solvent uptake compared to the unfilled ones [33].

In the study conducted by Takeuchi and Cohen in 1999, difunctional hydroxyl-terminated and vinyl-terminated poly (dimethyl siloxane) (PDMS) precursors with similar molecular weight distributions were used to synthesize end-linked networks in bulk with appropriate tetrafunctional cross-linkers. Composite PDMS elastomers from the same precursors were also synthesized with low concentrations of montmorillonite nanosize clay particles. For unfilled networks, larger amounts of tetraethyl orthosilicate (TEOS) cross-linkers than conventionally used led to optimal networks with higher moduli and lower soluble fractions. In the montmorillonite-PDMS elastomeric composites, enhancement of the modulus was obtained only for nonoptimal networks formed with the hydroxyl-terminated precursor chains but not with the vinyl-terminated chains. These results indicate that the reinforcement in these elastomers can be attributed to the anchoring of the hydroxyl end group of silicone to the silicate filler that dramatically reduces the soluble fraction and binds pendent chain ends. The modulus of the optimal networks could not be enhanced by clay reinforcement [34].

In 2000, Giannelis and Burnside investigated the relationship between structure and properties of polysiloxane-layered silicate nanocomposites. Solvent uptake (swelling) in dispersed nanocomposites was dramatically decreased as compared to

conventional composites, though intercalated nanocomposites and immiscible hybrids exhibited more conventional behavior. The swelling behavior is correlated to the amount of bound polymer (bound rubber) in the nanocomposites. Thermal analysis of the bound polymer chains showed an increase and broadening of the glass-transition temperature and loss of the crystallization transition. Both modulus and solvent uptake could be related to the amount of bound polymer formed in the system [35].

In 2010, Voulomenou and Tarantili prepared silicone rubber/organomontmorillonite (OMMT) nanocomposites and characterized their morphological, thermal, mechanical and swelling properties. Fourier transform infrared analysis, differential scanning calorimetry and thermogravimetric analysis did not show any significant effect of the nanofiller on the structural parameters of the composites, with the exception of a reduction in the crystallinity. Mechanical testing showed an improvement in the tensile strength and stiffness, whereas improved solvent resistance was recorded by swelling experiments in toluene. As a result, incorporation of OMMT into silicone rubber did not introduce any chemical changes but increased the density of crosslinks; this led to a loss of crystallinity, an increase in T_g , and a significant improvement in the tensile properties [37].

In 2011, Shirazi, Ghadimi and Mohammadi studied the pervaporation performance of PDMS nanocomposites. Different (PDMS) nanocomposite membranes were synthesized by incorporating various contents of nanosized silica particles to improve the PDMS pervaporation (PV) performance. According to the result of scanning electron microscopy (SEM) and atomic force microscopy (AFM), surface roughness increases by incorporating silica, and this decreases absorption of penetrants on the membrane. Swelling studies showed that the presence of silica nanoparticles into the PDMS membranes decreases degree of swelling, which can be attributed to rigidification of the PDMS matrix. Additionally, the results revealed that helium permeability decreases through the nanocomposite membranes, due to the more polymer chains packing. Effects of silica on recovery of isopropanol (IPA) from water mixtures were also investigated. Based on the results, incorporating silica nanoparticles promotes significantly the PDMS membrane selectivity because the polymer chains are rigidified and also the polymer free volume decreases. However, permeation flux decreases as diffusion of the penetrants reduces in the presence of

silica nanoparticles within the PDMS membranes. As PV performance depends on operating conditions, effects of feed composition, and temperature were also studied. Moreover, recoveries of IPA, ethanol, and methanol from water mixtures were compared using the PDMS-silica nanocomposite membranes. The results demonstrated that polarity and solubility of alcohols affect permeation flux and selectivity resulting in the higher permeation flux and selectivity for IPA [38].

In 2006, Schmidt, Clément and Giannelis investigated multi-system study of layered-silicate dispersion in polysiloxane/layered-silicate nanocomposites. A variety of layered silicates (montmorillonite, synthetic fluoromica, laponite, and fluorohectorite) and cationic modifiers (single-, twin- and triple-tailed surfactants with tails of varying lengths and both primary and quaternary head-groups) are combined to form organically modified layered silicates, which are then screened for compatibility with low-molecular-weight silanol-terminated poly (dimethyl siloxane) (PDMS). PDMS backbone is generally incompatible with the layered silicates, regardless of modification type, and that dispersion in PDMS systems results from the presence of polar end-groups, a result unprecedented in the field of polymer nanocomposites. In the absence of polar end-groups, dispersion was observed for poly (methylphenyl siloxane) but not poly(3,3,3-trifluoropropylmethyl siloxane). Application of a new epoxy/amine PDMS curing chemistry to PDMS-nanocomposite production showed higher levels of layered-silicate dispersion than silanol-terminated PDMS-based systems [39].

In 2012, Khanbabaee, Farahani and Rahmatpour studied on nanocomposite membranes of poly (dimethylsiloxane) (PDMS) with different amounts of fumed silica. Nanocomposite membranes were synthesized over a porous support of polyacrylonitrile. The prepared membranes were characterized using atomic force microscopy and thermal gravimetric analysis. AFM results indicated the nanoscale dispersion of silica particles in polymer matrix. TGA results indicated that increasing the silica content enhances the thermal stability of membranes. Permeation of methane and n-butane single gases at different upstream pressures and also permeation of a gas mixture containing 3 mol% of n-butane in methane were studied and discussed. The results showed that the nanocomposite membrane containing 11 wt% of fumed silica exhibited 38% increment in permeability of n-butane and simultaneously 30% increase in selectivity of n-butane over methane. The unusual

property enhancement that contradicts to that of conventional filled polymer systems has been discussed based on density of membranes and free volume concept [44].

In 2009 Lewicki, Liggat and Patel studied on thermal degradation of a series of novel poly (dimethyl siloxane)/montmorillonite (PDMS/MMT) nanocomposites. The thermal degradation behaviour of these nanocomposites was studied by means of thermal volatilization analysis (TVA) and thermogravimetric analysis (TGA). The major degradation products were characterized. The results demonstrate that the nanoclay significantly alters the degradation behaviour of the PDMS network, modifying the profile of the thermal degradation and reducing the overall rate of volatiles evolution. The results also indicate that the nanoclay promotes the formation of dimethylsilanone and benzene by inducing low levels of radical chain scission [53].

In 2009 Labruyere, Gorrasi, Monteverde, Alexandre and Dubois studied on PDMS/clay nanocomposites synthesized using a novel ω -ammonium functionalized oligo-PDMS surfactant (PDMS- $N^+(CH_3)_3$) and processed in membrane form. Morphological analysis and transport properties (sorption, diffusion and permeability) have been investigated using two penetrants: acetone and n-hexane. The mechanical and rheological properties of the PDMS nanocomposite membranes have also been studied. It has been found a significant effect of the clay organo-modifier on the morphology, physical and barrier properties of the systems [54].

3. EXPERIMENTAL

3.1 Chemicals

3.1.1 Poly (dimethyl siloxane) (PDMS)

PDMS was obtained from Dow Corning Corporation with a Silastic GP-30 Silicone Rubber trade name (Figure 2.11). This is vinyl-terminated amorphous silica whose specific gravity is 1.1 at 25 °C.

3.1.2 Bentonite

Bentonite was obtained from Eczacıbaşı Esan with 90.0 ± 5.0 meq/100gr cation exchange capacity and 80% montmorillonite mineral content. The chemical analysis of bentonite were measured and the results found as; 70% SiO₂, 13% Al₂O₃, 0.7% Fe₂O₃.

3.1.3 Hexadecyltrimethyl ammonium chloride (HDTMAC)

HDTMAC was obtained from Sigma Aldrich Co. with a $\geq 98.0\%$ purification and $M_w=320.00$ gmol⁻¹. It was used as modifier of bentonite.

3.1.4 (4-Carboxybutyl) triphenylphosphonium bromide (4CBTPPB)

4CBTPPB was also obtained from Sigma Aldrich Co. with a 98.0% and $M_w=443.31$ gmol⁻¹. It was used as modifier of bentonite.

3.1.5 Tributylhexadecylphosphonium bromide (TBHDPB)

TBHDPB was also obtained from Sigma Aldrich Co. with a 98.0% and $M_w= 507.67$ gmol⁻¹. It was used as modifier of bentonite.

3.1.6 Dicumyl peroxide

PEROXAN DC (dicumyl peroxide) was obtained from Pergan GmbH. It was used as cross-linking agent.

3.1.7 Toluene

Toluene was obtained from Tekkim Kimya San. Tic. Ltd. Şti. and used as solvent.

3.1.8 Chloroform

Chloroform was obtained from Tekkim Kimya San. Tic. Ltd. Şti. and used as solvent.

3.2 Equipments

3.2.1 Magnetic stirrer with heater

IKA RCT Standard model magnetic stirrer with heater has a maximum mixing rate of 1500 rpm and it can be heated to a maximum temperature of 350 °C.

3.2.2 Vacuum oven

Nüve EV 018 model vacuum oven can be heated to a maximum temperature of 200 °C

3.2.3 Ultrasonic bath

Everest CleanEx model ultrasonic bath has 4 lt. water volume and 240 watt ultrasonic power.

3.2.4 Fourier transform infrared spectroscopy (FTIR) test device

Perkin Elmer Spectrum 100 model FTIR apparatus with ATR (Attenuated Total Reflectance) technique was used to determine the organic components of the samples. % transmittance versus wavenumber graph was obtained from the apparatus.

3.2.5 X-ray diffraction (XRD) analysis

Rigakku, Miniflex 2, Japan X-ray Diffractometer with CuK α radiation ($\lambda = 1.5418\text{Å}$), 45kV/40mA was used.

3.2.6 Thermogravimetric analysis (TGA) test device

Exstar SII TG/DTA 7200 model thermogravimetric analysis test device was used. Instrument has a maximum temperature of 1100 °C with 0.2 μg TG sensitivity and 0.01 to 150 °C/min scan rate. Samples were analyzed in N₂ atmosphere.

3.2.7 Mechanical test device

Instron 3345 model universal test machine with 5kN capacity was used to determine the mechanical properties of polymer nanocomposites. Tensile test gives an instantaneous load F (N) versus elongation (mm) chart which is converted into engineering stress σ (MPa) and engineering strain ϵ (mm/mm) by using the initial gauge length, which is the length of the center section, and initial cross sectional area A_0 .

3.2.8 Dynamic mechanical analysis (DMA) test device

Metravib DMA50 model dynamic mechanical analysis equipment was used to determine the storage, loss and complex modulus values of the samples.

3.2.9 Shore-A hardness test device

Zwick Roell Shore A in accordance with ASTM D 2240 was used.

3.2.10 Contact angle test device

Attension Biolin Scientific AB, ThetaLite TL101 model optical tensiometer apparatus was used to measure contact angles of the surfaces.

3.2.11 Field emission-scanning electron microscopy (FE-SEM) test device

Field-Emission Scanning Electron Microscopy (FE-SEM) (SUPRA 35VP, LEO-Gemini, GmbH, Germany) was employed.

3.3 Experimental Procedure

3.3.1 Modification of bentonite

For the preparation of phosphonium and ammonium modified bentonites; firstly, the pure bentonites were dried in vacuum at 60°C for 12 h. The amounts of the surfactants added to all clays were 1.5 times the CEC. 5 g of clay were put into 150 ml of w/w 50:50 distilled water: ethanol solution at room temperature, in an erlenmeyer flask equipped with a mechanical stirring bar. System was heated till it reached 80 °C. After 4 h, mixing was stopped and then the organo-montmorillonite was precipitated by centrifuge at 5000 rpm and 5 minutes. Washing was repeated for at least six times till no halide traces were detected with silver nitrate by repeating centrifuge step. After washing, the organically modified bentonite was dried

overnight at room temperature followed by drying at 80°C for 24 h under vacuum. Thus they were grounded.

3.3.2 PDMS nanocomposites preparation

According to the modifier type PDMS was solved in the suitable solvent over night. 3% by weight of the dicumyl peroxide was added into the PDMS solution and then 3-5-10% by weight of the organo-clay was added and mixed mechanically about 2 hours. This blend was then sonicated for 45 minutes in order to exfoliate the clay platelets. The resin blend was degassed in the vacuum oven by just using the vacuum pump. The mixture was transferred into the Teflon® mould. Solvent was evaporated at room conditions then finally, put into the oven at about 180 °C to be cured.

3.4 Characterization

3.4.1 Fourier transform infrared spectroscopy (FTIR)

FTIR analysis was performed over the range of 400 to 4000 cm^{-1} at room conditions. Samples were prepared to determine the organic components in the samples. Pure bentonite (B) and organically modified bentonites (HDTMAC-B, TBHDPB-B and 4CBTPPB-B) were characterized for the comparison. PNCs were also characterized.

3.4.2 X-ray diffraction (XRD) analysis

XRD technique is an important field of application is the identification of crystalline fractions in samples. Equipment was used for structural analyses of the pure bentonite (B), modified bentonites (HDTMAC-B, TBHDPB-B and 4CBTPPB-B) and all concentrations such as 3-5-10% of PDMS-organoclay nanocomposites. XRD patterns of the samples were recorded by monitoring the diffraction angled (2θ) from 2° to 12° . Samples were determined by using XRD equipment at 40 kV, 40 mA with $\text{CuK}\alpha$ radiation ($\lambda=1.5414\text{\AA}$). Basal distance of the layers (d) were calculated by using Bragg equation ($n\lambda=2.d.\sin\theta$). In the equation, λ (\AA) is the wavelength of the x-ray, θ ($^\circ$) is the scattering angle, and n is an integer representing the order of the diffraction peak.

3.4.3 Thermogravimetric analysis (TGA)

Thermal gravimetric analysis (TGA) of the pure PDMS and PDMS/organoclay nanocomposites were carried out by using Exstar SII TG/DTA 7200 thermal gravimetric analyzer from 30°C to 1000°C at a heating rate 10 °C/min. Nitrogen was used as a carrier gas with a constant flow rate during analysis.

3.4.4 Tensile test

From the measured stress and strain values, elongation at break, stress at break, E-modulus were calculated from the average of at least 5 specimens tested. Specimens were cut with a cutter in accordance with the ASTM E-8 Standard. For the comparing of the mechanical improvements on thePNCs, mechanical properties of cross-linked pure PDMS were measured andcalculated. 500 mm/min constant elongation speed was used for the measurements with 5kN capacity to obtain the response of the prepared nanocomposites to the applied force and the extent to which the specimens elongate before failure.

3.4.5 Dynamic mechanical analysis (DMA)

Dynamic oscillation is one of the most popular means to determine the viscoelastic response of materials. Storage modulus (E'), loss modulus (E'') and absolute value of modulus ($|E|$) of the samples were measured in the frequency range 1-200 Hz at constant temperature 25 ± 2 °C.

3.4.6 Shore-A hardness test

Accordingto standard measurement (ASTM D 2240); after 3 seconds and 20 seconds of the beginning the measured values were recorded. For every sample, at least 3 parallel values measuredand the averages of the values were calculated and recorded.

3.4.7 Contact angle measurements

Various types of liquids such as deionized water, diiodomethane and ethylene glycol were used to measure the contact angles of the PDMS nanocomposites in order to calculate surface free energy and determine surface behavior. The sessile drop method was applied.Contact angle values that are smaller than 90° indicate surface hydrophilicity.

Young's equation is used to calculate contact angle.

Young's equation:

$$\gamma_S = \gamma_{SL} + \gamma_{LV} \cos\theta \quad (3.1)$$

Owen-Wendt equation:

$$\gamma_{SL} = \gamma_S + \gamma_{LV} - 2\sqrt{\gamma_S^D \gamma_{LV}^D} - 2\sqrt{\gamma_S^P \gamma_{LV}^P} \quad (3.2)$$

The following equation is reduced by using above mentioned two equations.

$$\frac{1 + \cos\theta}{2} x \frac{\gamma_{LV}}{\sqrt{\gamma_{LV}^D}} = \sqrt{\gamma_S^P} x \sqrt{\frac{\gamma_L^P}{\gamma_L^D}} + \sqrt{\gamma_S^D} \quad (3.3)$$

γ is surface free energy and the subscripts of S , L and V mean solid, liquid and vapor phases, respectively. γ^P and γ^D also represent polar and dispersive forces at the solid surface to give a resultant surface free energy, respectively. And the sum of both γ^P and γ^D equal to γ [48-51].

3.4.8 Field emission-scanning electron microscopy (FE-SEM)

Field Emission Scanning Electron Microscopy was used to examine the morphology of the fractured samples by applying carbon coatings. The distributions of P (phosphorus) in PDMS nanocomposite samples were investigated by the mapping results obtained from SEM-EDX analysis.

Under vacuum, electrons generated by a Field Emission Source are accelerated in a field gradient. The beam passes through electromagnetic lenses, focussing onto the specimen. As result of this bombardment different types of electrons are emitted from the specimen. A detector catches the secondary electrons and an image of the sample surface is constructed by comparing the intensity of these secondary electrons to the scanning primary electron beam. Finally the image is displayed on a monitor [45].

4. RESULTS AND DISCUSSION

Ammonium salts, which are most frequently applied, suffer from thermal degradation during the fabrication and further processing of nanocomposites. This leads to changes in the surface properties of clays resulting in alteration of nanocomposite structure and the contamination of polymeric material with the products of thermal degradation of an organic modifier, which may be responsible for enhanced thermal degradation of the polymer matrix, accelerated aging color formation, plasticization effects, and so forth. Due to the limited thermal stability of ammonium salts and being high temperature material of PDMS; current efforts focus on selecting new clay modifiers that display significantly higher thermal stability than ammonium compounds, provide effective modification of the polymer/clay interface, and facilitate clay dispersion.

In this study, cross-linked PDMS nanocomposites were prepared by using alkyl ammonium and alkyl phosphonium modified bentonites with varying compositions such as 3-5-10%. The modification of bentonite and the preparation conditions of nanocomposites were given in section 3.3.1 and 3.3.2 respectively. The modifiers were selected according to their structures. One type of ammonium salt and two types of phosphonium salts were selected for comparison of their structure effect to polymer matrix. Hexadecyltrimethylammonium chloride, tributylhexadecylphosphonium bromide and (4-carboxybutyl) triphenylphosphonium bromide were selected. Their main differences are; 1) to compare ammonium and phosphonium salt; 2) to compare alkyl and phenyl group containing salts.

The cross-linked PDMS without organoclay was also prepared for the comparison purposes. The prepared thirteen samples were characterized.

The need to improve the thermal stability of organoclays applied in the preparation of polymeric nanocomposites has motivated the search for an organic modifier

combining high thermal stability with high efficiency in facilitating dispersion of nanofiller in a polymer matrix.

4.1 FTIR Results

FTIR analysis was used to examine the chemical composition and structure of materials. In this study, pure bentonite (B), organically modified bentonites (HDTMAC-B, TBHDPB-B and 4CBTPPB-B) and cross-linked PDMS nanocomposites were characterized to obtain FTIR spectra. The structural and characteristic groups of materials were determined. FTIR spectra were recorded in the absorbance mode. The FTIR spectra of samples were presentend in Figure 4.1.

In the FTIR spectra of cross-linked pure PDMS and PDMSNCs (Figure 4.1) the band at 2963 and 2905 cm^{-1} refer to CH stretching region of CH_3 . While the bands at 1446 and 1412 cm^{-1} show CH_3 asymmetric deformation of Si-CH_3 , the band at 1258 cm^{-1} shows CH_3 symmetric deformation of Si-CH_3 . The peaks at 1007 cm^{-1} and shoulder at 1091 cm^{-1} refer to Si-O-Si stretching vibrations. Si-C stretching and CH_3 rocking are shown at the peaks 863 and 787 cm^{-1} . These results are in aggrement with references [46]

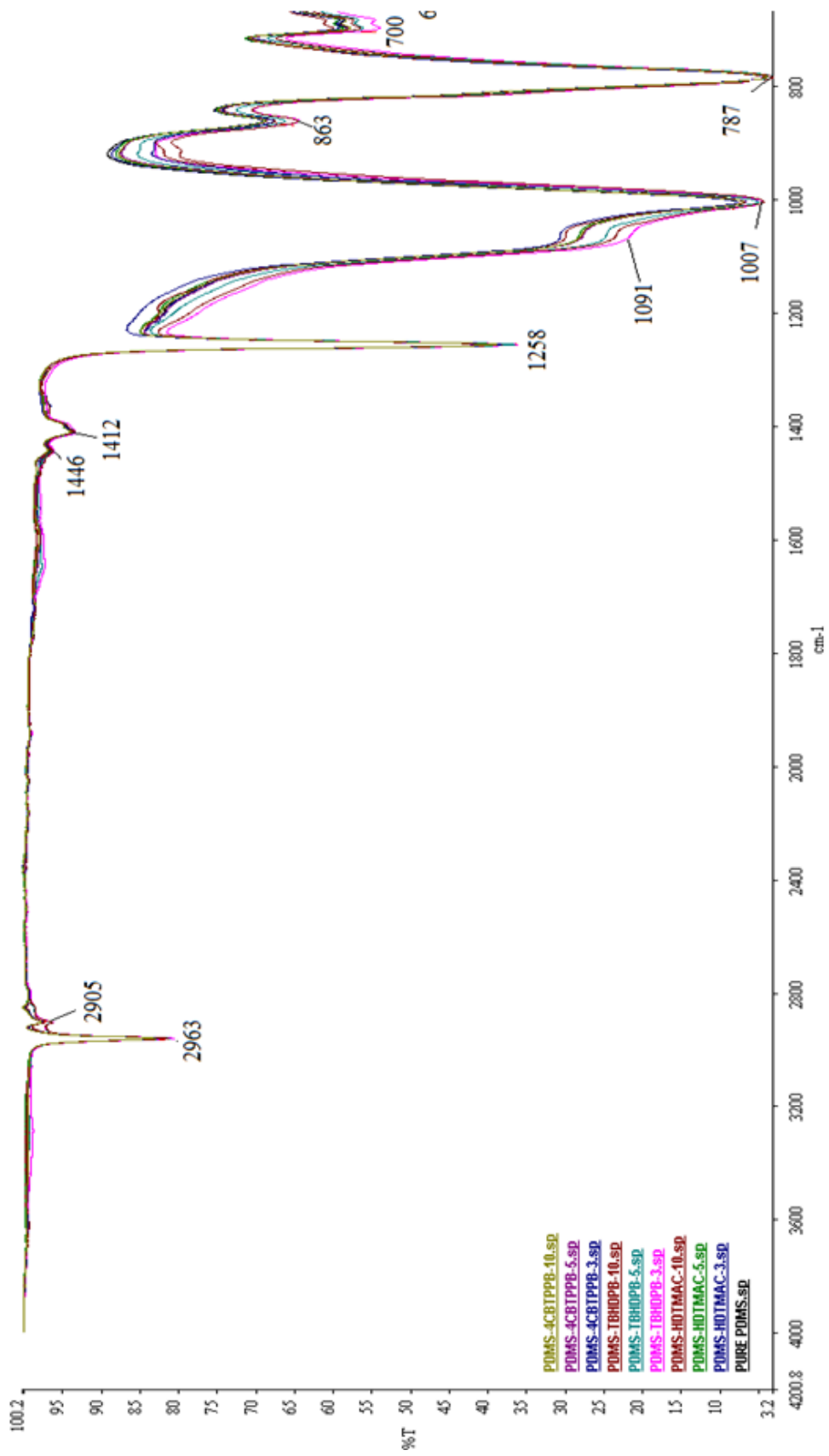


Figure 4.1 : FTIR spectra of the cross-linked pure PDMS and PDMSNCs.

4.2 XRD Analysis Results

To analyze the dispersion state of an organoclay in the polymer matrix and the interlayer spacing of the silicate layers XRD is a useful technique. The patterns obtained from the analysis are used for the characterization of the structure of nanocomposites by using the 2 θ peak, which is used for the calculation of the distance between the silicate layers with Bragg's law. The intercalation of polymer chains between the silicate layers results in an increase in the interlayer spacing. For those intercalated structures; the characteristic peak tends to shift to a lower angle due to the expansion of the basal spacing. Although the layer spacing increases, there still exists an attractive force between the layers to stack them in an ordered structure. Change in intensity and the shape of the basal reflections is another evidence that specifies the intercalation of polymer chains.

On the contrary, no peak can be observed in the XRD pattern of exfoliated polymer nanocomposites owing to fully dispersed clay platelets in the matrix. The absence of a diffraction peak may indicate an exfoliated or delaminated structures, however, it should not be used as the only evidence for the formation of an exfoliated structure. Due to the low concentration of the organoclay, X-ray beams may hit to a non-uniformly dispersed region of the sample and Bragg's reflection may be eliminated demonstrating exfoliation or it may remain unchanged as conventional structures.

The XRD patterns of the clays, raw bentonite (B), modified bentonites with hexadecyltrimethylammonium chloride (HDTMAC-B), tributylhexadecylphosphonium bromide (TBHDPB-B) and (4-carboxybutyl) triphenylphosphonium bromide (4CBTPPB-B), used in this study were obtained. The basal spacing values determined from Bragg equation (assuming the order of the diffraction peak (n) as 1) of raw bentonite, organoclay and nanocomposites are shown in Table 4.1. The basal spacing of the unmodified bentonite and organically modified bentonites B, HDTMAC-B, TBHDPB-B and 4CBTPPB-B are found as 13,86Å, 19,47Å, 24,27 Å and 20,02Å respectively that can be seen in Figure 4.2.

Table 4.1 : XRD results of the pure bentonite, organoclays and PDMS/organoclay nanocomposites

Samples	2theta (°)	d ₀₀₁ (Å)
B	7.08	13.86 Å
HDTMAC-B	4.97	20.02 Å
TBHDPB-B	3.98	24.27 Å
4CBTPPB-B	5.04	19.47 Å
PDMS- HDTMAC-B-3	<2	>44.04 Å
PDMS- HDTMAC -B-5	<2	>44.04 Å
PDMS- HDTMAC-B-10	<2	>44.04 Å
PDMS-TBHDPB-B-3	<2	>44.04 Å
PDMS-TBHDPB-B-5	<2	>44.04 Å
PDMS-TBHDPB-B-10	<2	>44.04 Å
PDMS-4CBTPPB-B-3	<2	>44.04 Å
PDMS-4CBTPPB-B-5	<2	>44.04 Å
PDMS-4CBTPPB-B-10	<2	>44.04 Å

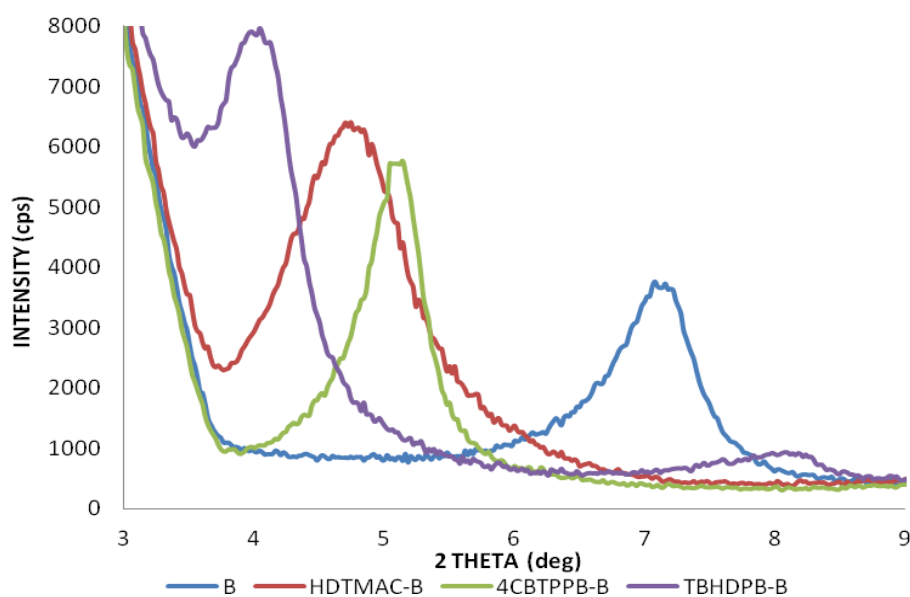


Figure 4.2 : XRD pattern of the pure bentonite and bentonites modified with HDTMAC, TBHDPB and 4CBTPPB.

As seen from the results, modification of the pure bentonite with HDTMAC, TBHDPB and 4CBTPPB causes an increase in the basal distance of planes about 40-45% ratios. XRD patterns of their nanocomposites with PDMS are presented in Figure 4.3, Figure 4.4 and Figure 4.5. There is no peak in the charts. So, exfoliated polymer nanocomposites were obtained.

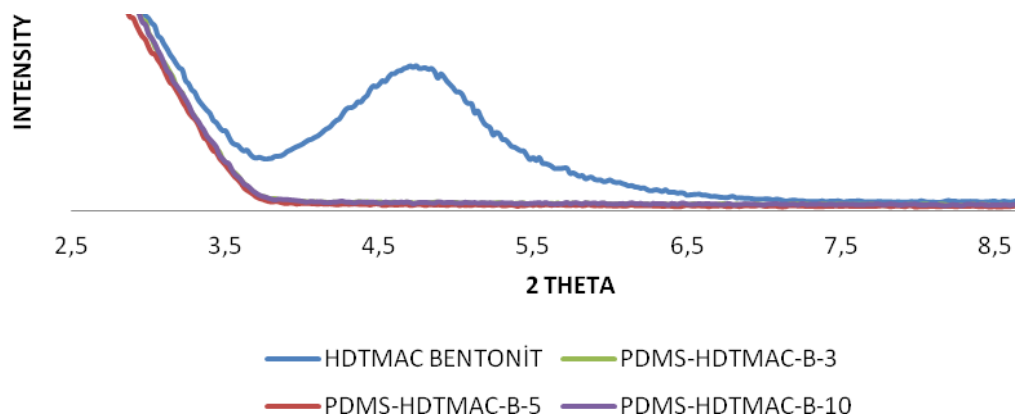


Figure 4.3 : XRD pattern of the organoclay modified with HDTMAC and its PDMS/organoclay nanocomposite with 3-5-10% contents

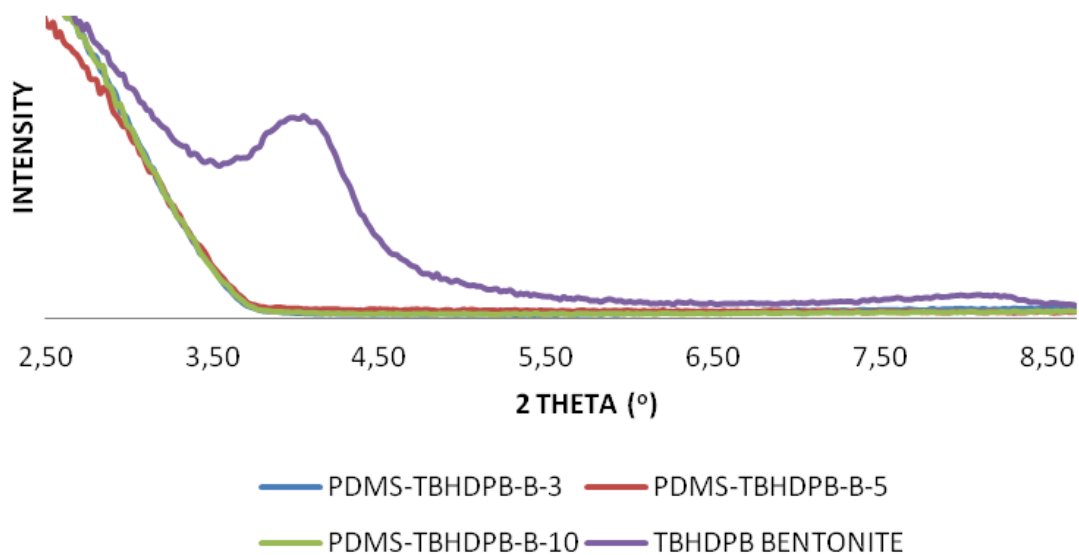


Figure 4.4 : XRD pattern of the organoclay modified with TBHDPB and its PDMS/organoclay nanocomposite with %3-5-10 contents

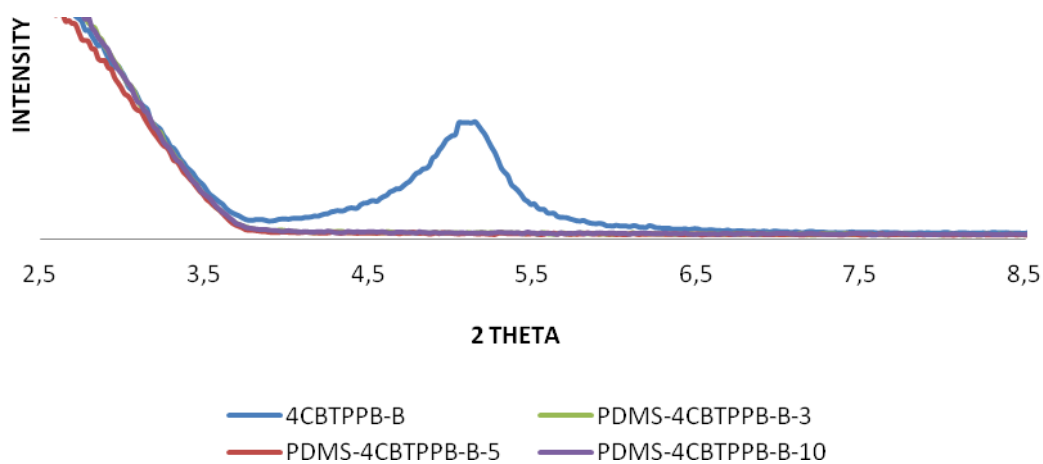


Figure 4.5 : XRD pattern of the organoclay modified with 4CBTPPB and its PDMS/organoclay nanocomposite with %3-5-10 contents

4.3 TGA Results

The thermal gravimetric analyses of pure bentonite, modified bentonites with HDTMAC, TBHDPB, 4CBTPPB and cross-linked pure PDMS, PDMS/organoclay nanocomposites were performed in order to investigate the effects of salts used on the clay and the resulting nanocomposites.

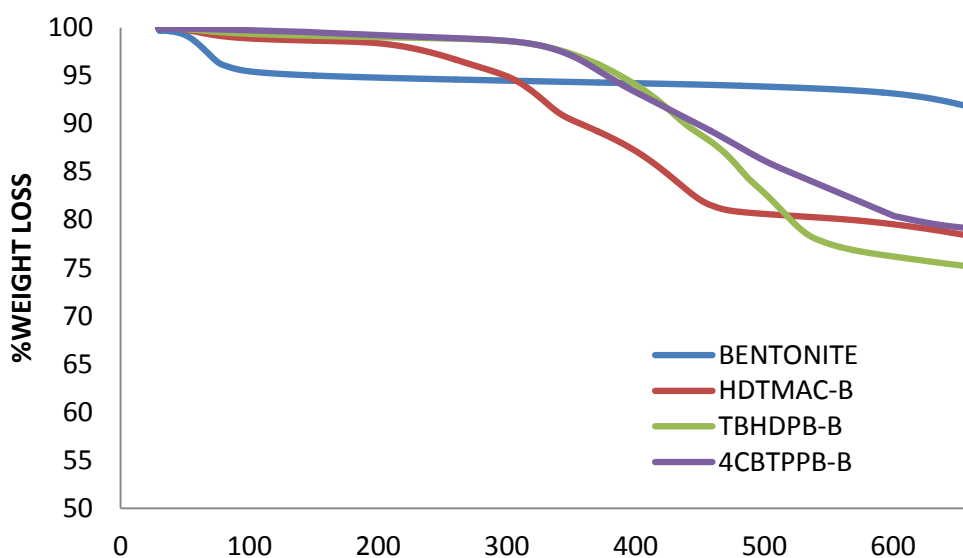


Figure 4.6 : TGA thermograms of the pure bentonite and organically modified bentonites

TGA results of pure bentonite, HDTMAC modified bentonite, TBHDPB modified bentonite and 4CBTPPB modified bentonite were given in Figure 4.6. All samples were characterized at the same conditions. The weight loss between 50 and 150 °C, corresponding to the evaporation of water and solvent molecules. Unmodified bentonite is hydrophilic material. So that; pure bentonite had humidity in its structure although the samples were dried before the characterization. Organically modified bentonite became hydrophobic structure after the modification.

According to Figure 4.7 and Figure 4.8 onset decomposition temperatures of pure PDMS, PDMS-HDTMAC-B-5, PDMS-TBHDPB-B-5 and PDMS-4CBTPPB-B-5 are determined as 491,8 °C, 499,12 °C, 493,31°C and 516,82 °C respectively. As seen at small chart in Figure 4.6 pure PDMS starts to decompose at very low temperature until the weight loss reached to 4% shown in Figure 4.8, then PDMS-HDTMAC-B-5 nanocomposite decomposes before pure PDMS and PDMS-4CBTPPB-B-5 at elevated temperatures. After the decomposition finishes, the amount of the char % of

the pure PDMS, PDMS-HDTMAC-B-5, PDMS-TBHDPB-B-5 and PDMS-4CBTPPB-B-5 are 24, 27.5 %, 27% and 27% at the temperature of 598, 584, 587. and 596 °C respectively.

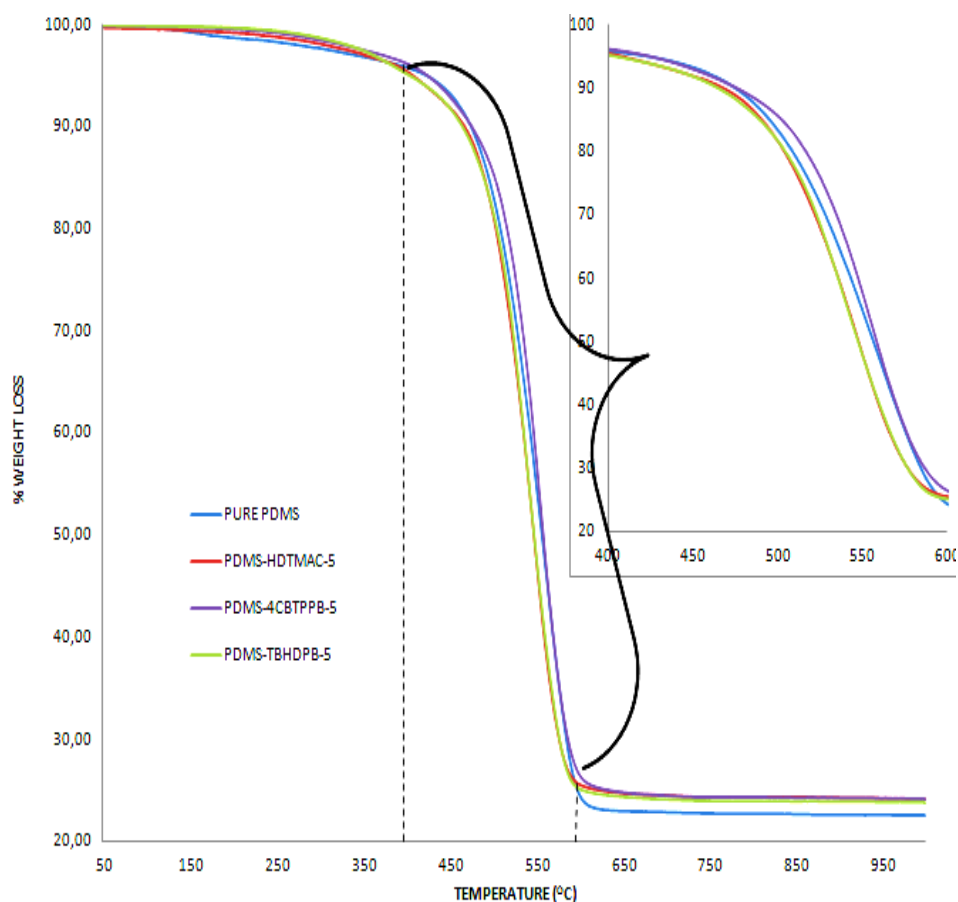


Figure 4.7 : TGA thermograms of the cross-linked pure PDMS, PDMS-HDTMAC-B-5, PDMS-TBHDPB-B-5 and PDMS-4CBTPPB-B-5

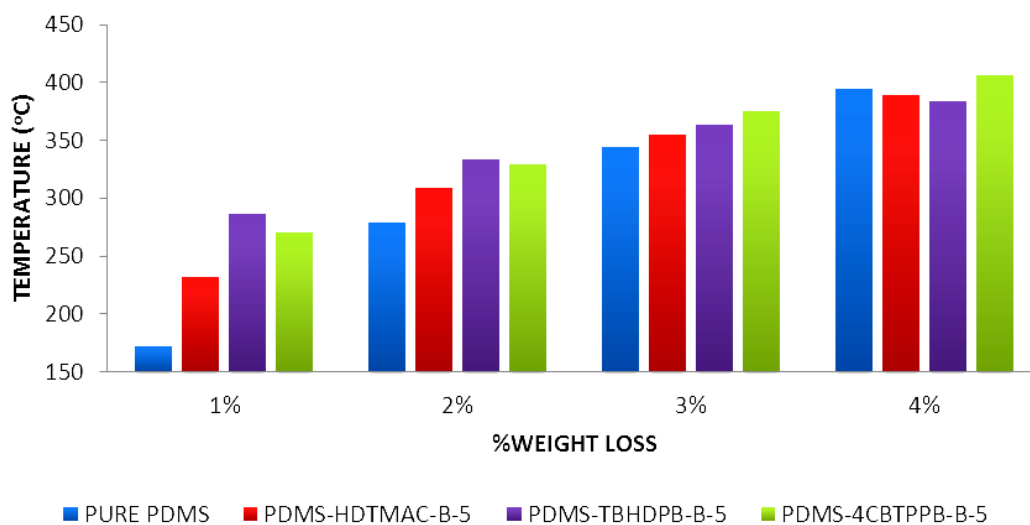


Figure 4.8: Decomposition temperatures until the 4% weight loss of the materials

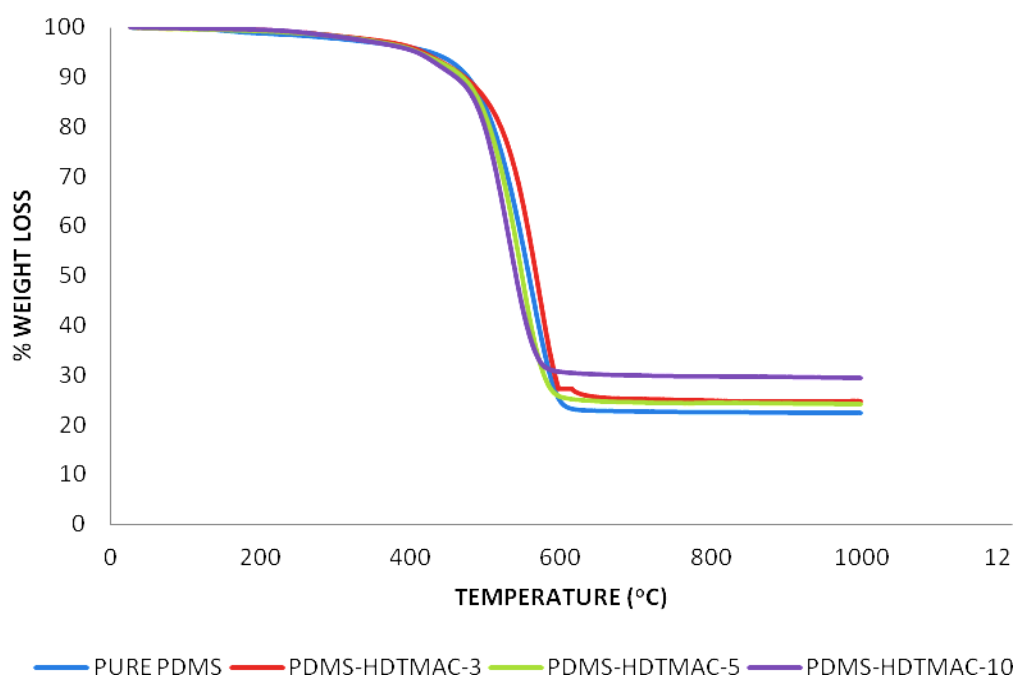


Figure 4.9 : TGA thermogram of the PDMS-HDTMAC-B-3, PDMS-HDTMAC-B-5 and PDMS-HDTMAC-B-10

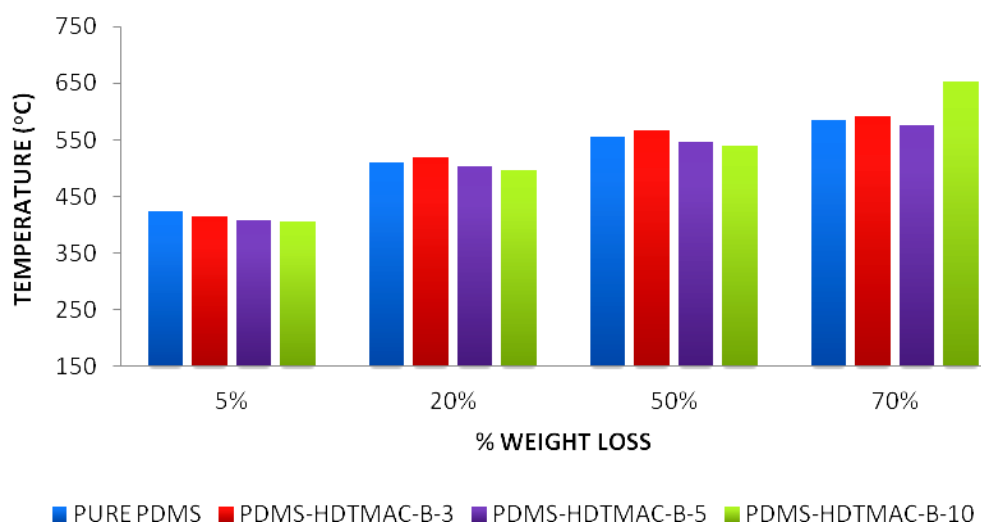


Figure 4.10 : Percent weight loss versus temperature comparison of the pure-PDMS, PDMS-HDTMAC-B-3, PDMS-HDTMAC-B-5 and PDMS-HDTMAC-B-10

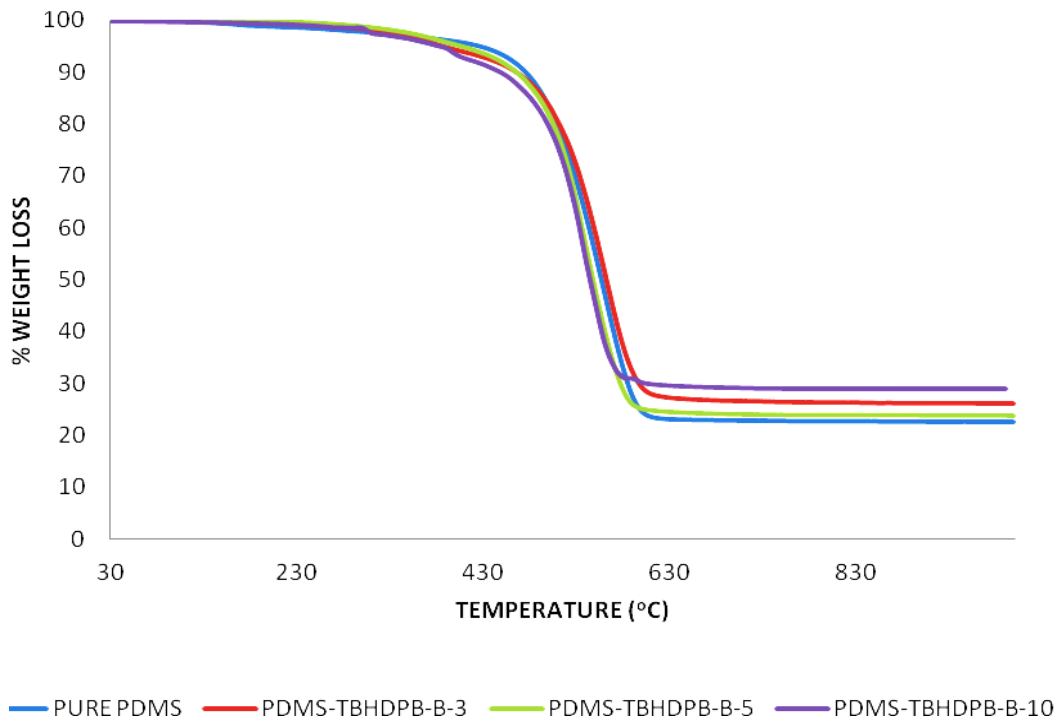


Figure 4.11 : TGA thermogram of the PDMS-TBHDPB-B-3, PDMS-TBHDPB-B-5 and PDMS-TBHDPB -B-10

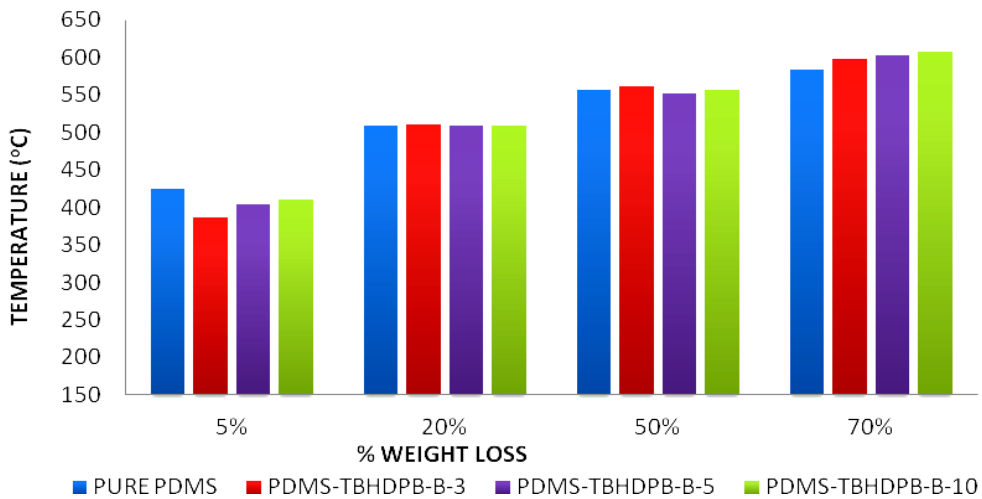


Figure 4.12 : Percent weight loss versus temperature comparison of the pure-PDMS, PDMS-TBHDPB-B-3, PDMS-TBHDPB-B-5 and PDMS-TBHDPB-B-10

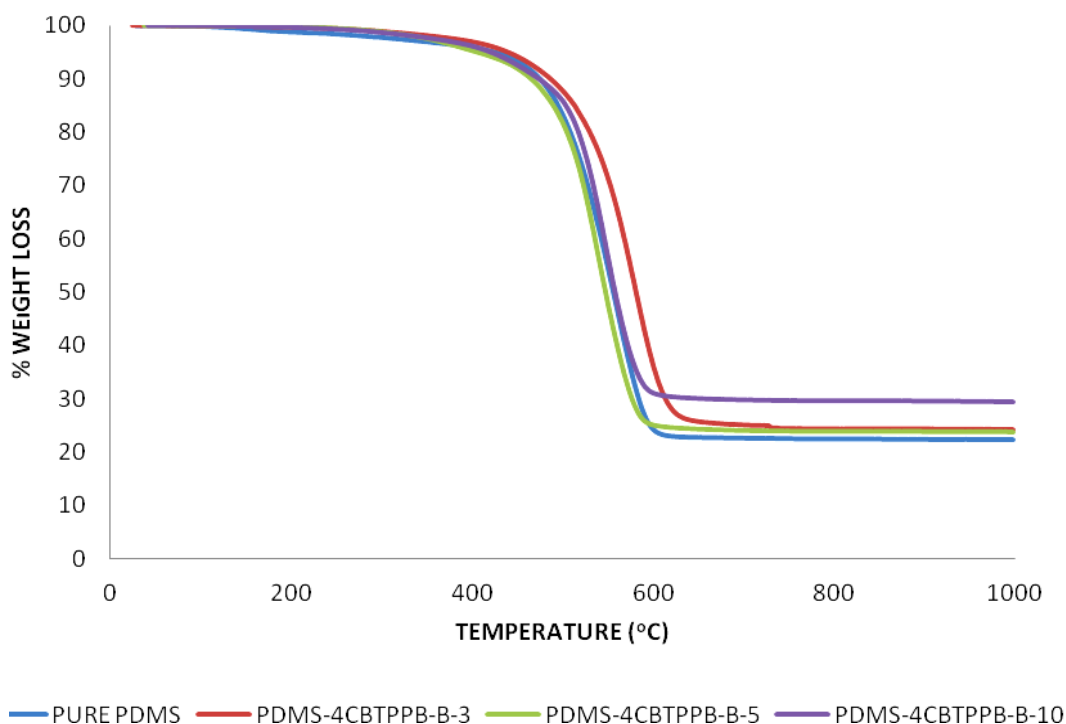


Figure 4.13: TGA thermogram of the PDMS-4CBTPPB-B-3, PDMS-4CBTPPB-B-5 and PDMS-4CBTPPB-B-10

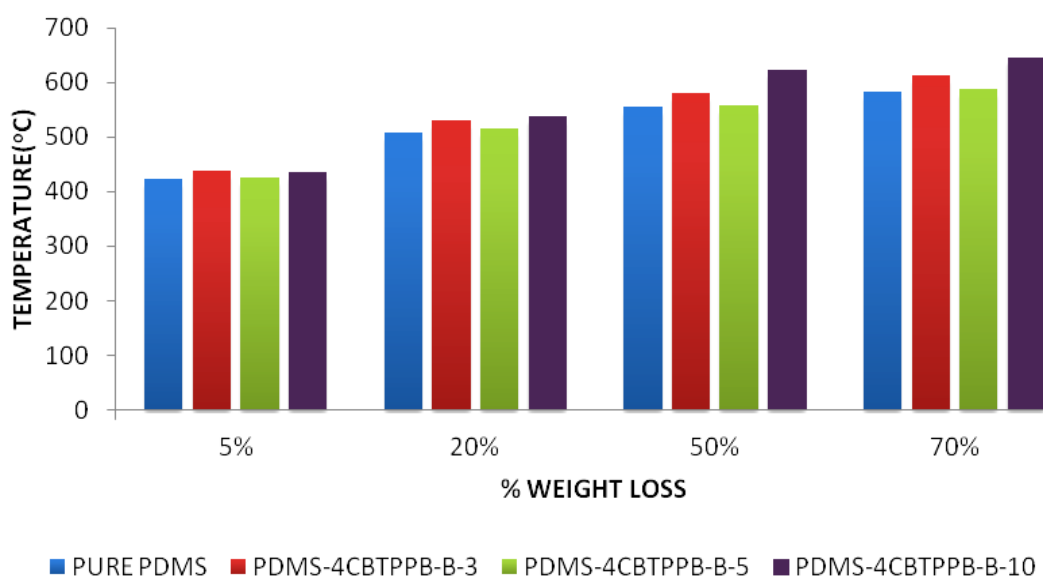


Figure 4.14 : % Weight loss versus temperature comparison of the pure-PDMS, PDMS-4CBTPPB-B-3, PDMS-4CBTPPB -B-5 and PDMS-4CBTPPB-B-10

According to the TGA test results, decomposition temperatures of PDMS-4CBTPPB-B nanocomposites were increased with comparison of decomposition temperatures of PDMS-HDTMAC-B and PDMS-TBHDPB-B nanocomposites due to the existing phenyl groups in the structures.

4.4 Tensile Test Results

Tensile tests were performed with universal test machine to measure the elastic modulus and the tensile strength with elongation at break values from the stress-strain curves. The tensile properties of the materials are shown in Table 4.2, Table 4.3 and Table 4.4. E-modulus values of the samples were increased about 19.6%. Whereas 3% organoclay content was not effective on E-modulus results, 5 and 10% organoclay content enhances.

Table 4.2 : Tensile test results of the pure PDMS and PDMS-4CBTPPB-B nanocomposite with varied contents of organoclays

Clay Content	PDMS-4CBTPPB-B		
	Tensile Strength (MPa)	Elongation at Break (%)	E-Modulus (MPa)
0%	5.51	958	1.07
3%	3.51	664	1.08
5%	5.17	786	1.20
10%	5.89	1028	1.28

Table 4.3 : Tensile test results of the pure PDMS and PDMS-HDTMAC-B nanocomposite with varied contents of organoclays

Clay Content	PDMS-HDTMAC-B		
	Tensile Strength (MPa)	Elongation at Break (%)	E-Modulus (MPa)
0%	5.51	958	1.07
3%	6.04	1063	0.98
5%	5.65	1061	1.19
10%	6.16	1456	1.22

Table 4.4 : Tensile test results of the pure PDMS and PDMS-TBHDPB-B nanocomposite with varied contents of organoclays

Clay Content	PDMS-TBHDPB-B		
	Tensile Strength (MPa)	Elongation at Break (%)	E-Modulus (MPa)
0%	5.51	958	1.07
3%	5.09	810	1.06
5%	5.66	1181	1.24
10%	5.36	975	1.29

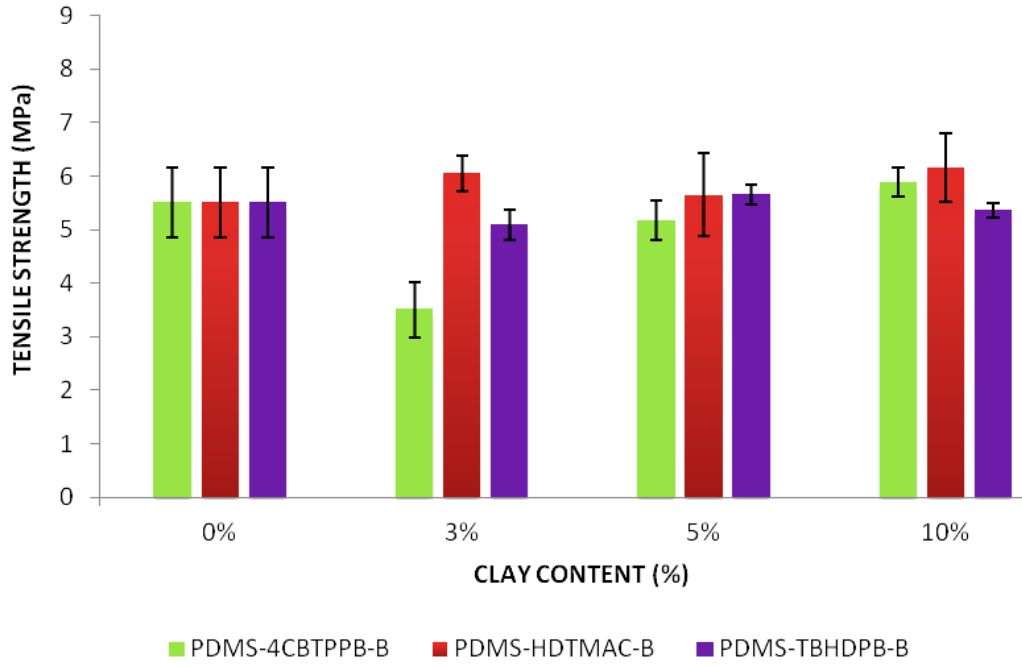


Figure 4.15 : Tensile strength results of PDMS-4CBTPPB-B, PDMS-TBHDPB-B and PDMS-HDTMAC-B with varied contents

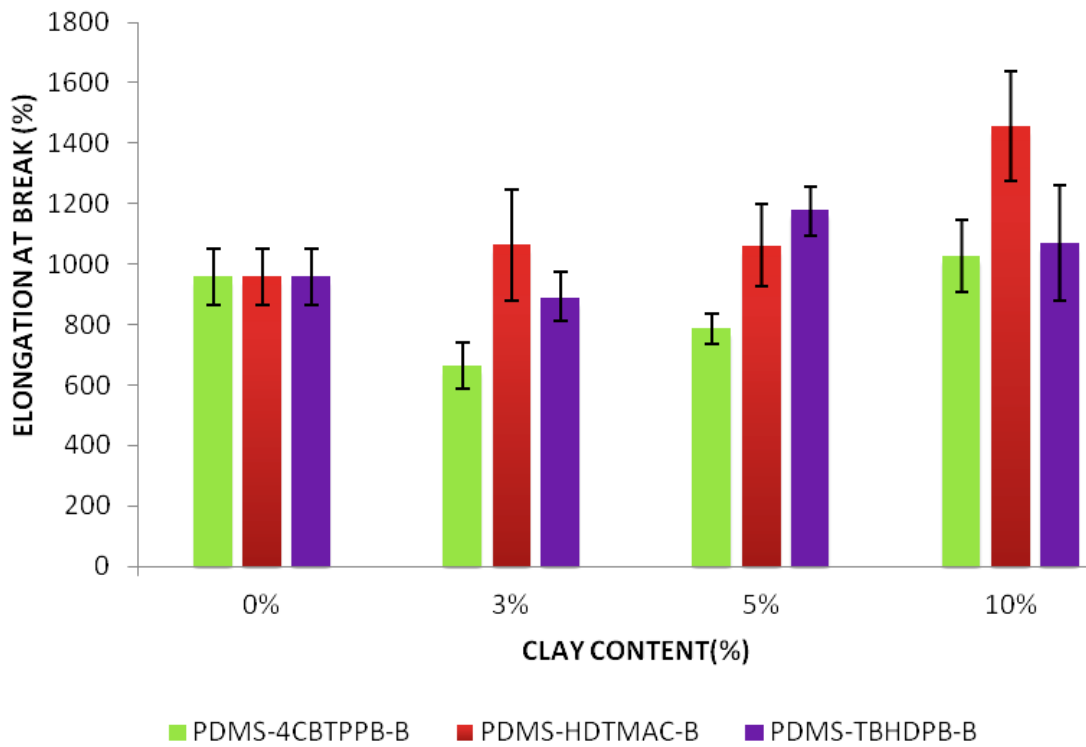


Figure 4.16 : Elongation at break results of PDMS-4CBTPPB-B, PDMS-HDTMAC-B and PDMS-TBHDPB-B with varied contents

4.5 DMA Test Results

Frequency sweeps are oscillatory tests performed at variable frequencies, keeping the amplitude (and also the measuring temperature) at a constant value. Sometimes, the term “dynamic oscillation” is used as a synonym for “variable frequencies” (as in ASTM D4440). Frequency sweeps are used to investigate time-dependent behaviour since the frequencies the inverse value of time. Short-term behaviour is simulated by rapid motion (i.e., at high frequencies) and long-term behaviour by slow motion (i.e., at low frequencies) [47].

In this study, the frequency sweep was applied to the PDMSNCs to obtain storage modulus (E'), loss modulus (E'') in the frequency range 1-200 Hz at constant temperature 25 ± 2 °C. Then absolute value of the modulus ($|E|$) was calculated for every value as given below:

$$E = \sqrt{E'^2 + E''^2} \quad (4.1)$$

Table 4.5 :Storage modulus (E') results of PDMSNCs

Frequency (Hz.)	PURE PDMS (MPa)	PDMS-HDTMAC (MPa)			PDMS-TBHDPB (MPa)			PDMS-4CBTBPB (MPa)		
		3%	5%	10%	3%	5%	10%	3%	5%	10%
1	1.89	6.27	3.46	2.44	1.36	1.20	2.93	1.70	2.14	2.06
2.13	1.48	6.73	2.98	3.05	1.85	1.70	3.51	2.17	2.60	2.57
4.54	1.05	7.18	2.48	3.60	2.25	2.19	4.05	2.56	3.06	3.03
9.68	1.01	7.21	2.53	3.76	2.20	2.26	4.19	2.57	3.04	3.09
44.01	10.3	13.1	13.1	14.52	7.43	7.21	5.38	6.96	6.47	6.29
93.82	41.6	30.7	48.9	33.6	40.6	40.4	37.8	39.5	38.2	39.1
200	218	211	252	202	216	221	225	224	223	221

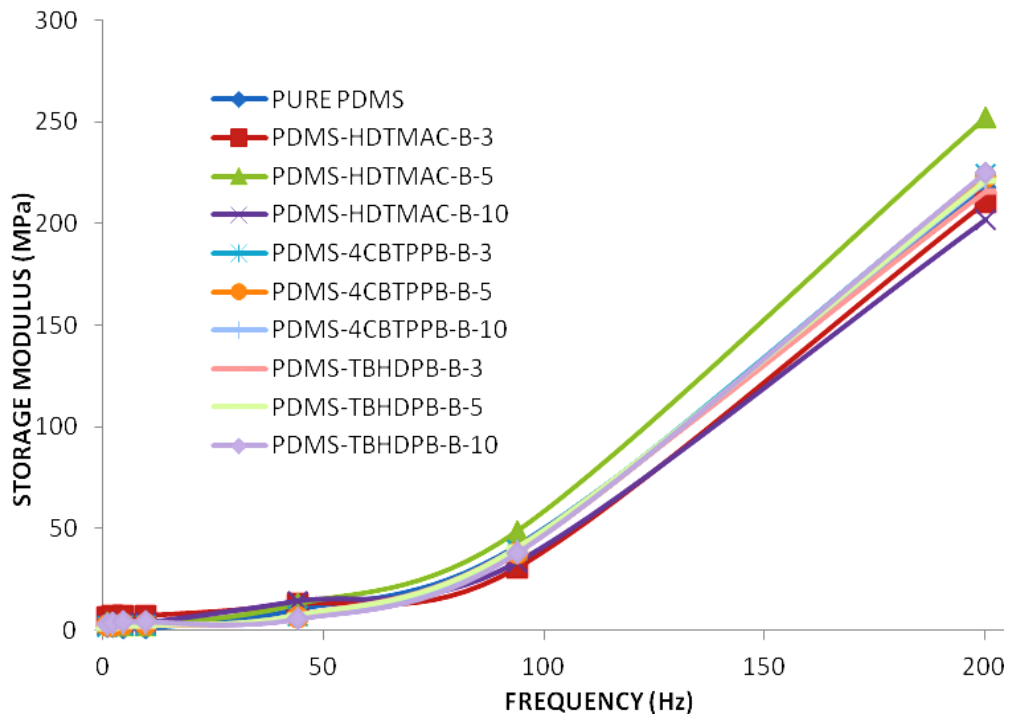


Figure 4.17 : Frequency versus storage modulus (E') results of PDMSNCs

Table 4.6: Loss modulus (E'') results of PDMSNCs

Frequency (Hz.)	PURE PDMS (MPa)	PDMS-HDTMAC (MPa)			PDMS-TBHDPB (MPa)			PDMS-4CBTBPB (MPa)		
		3%	5%	10%	3%	5%	10%	3%	5%	10%
1	1.67	0.08	1.92	0.85	0.47	0.63	0.75	0.63	0.55	0.58
2.13	1.66	0.09	1.93	0.92	0.47	0.67	0.80	0.56	0.54	0.63
4.54	1.67	0.1	1.92	0.97	0.50	0.72	0.91	0.62	0.65	0.73
9.68	1.65	0.2	1.85	1.05	0.55	0.80	0.93	0.63	0.62	0.73
44.01	2.59	0.46	2.90	0.39	1.21	1.55	2.07	0.104	0.149	0.017
93.82	12.2	9.51	13.9	8.1	9.61	9.46	9.02	9.53	9.53	9.30
200	71.3	69.34	79.2	63.62	67.63	73.7	74.4	67.64	73.25	70.07

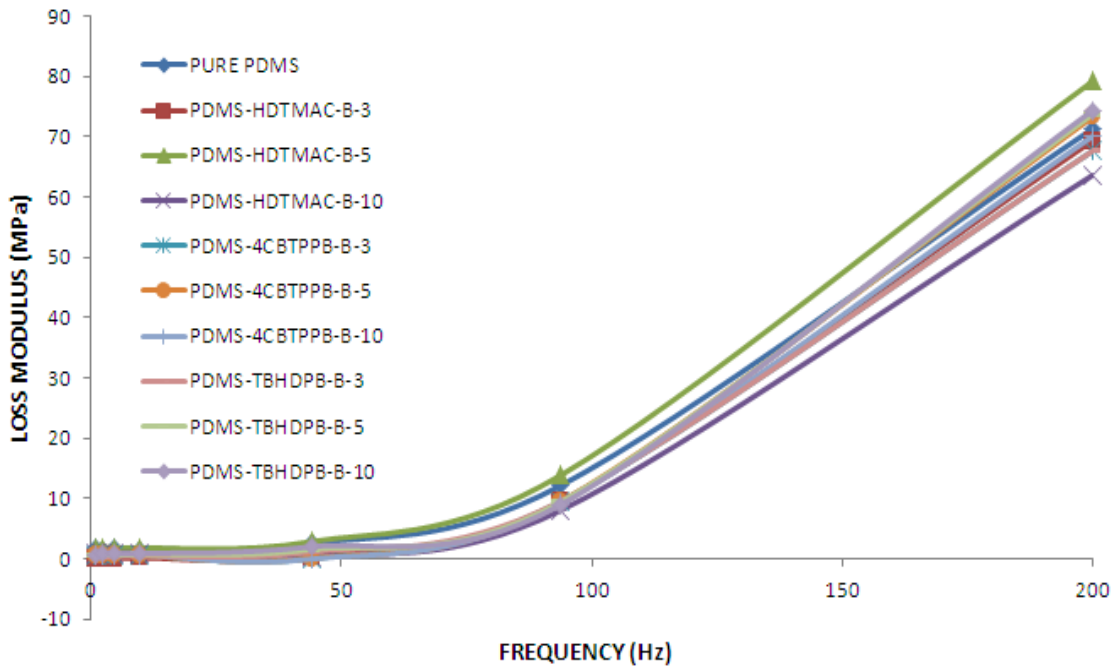


Figure 4.18 : Frequency versus loss modulus (E'') results of PDMSNCs

Table 4.7: Absolute value of the modulus ($|E|$) results of PDMSNCs

Frequency (Hz.)	PURE PDMS (MPa)	PDMS-HDTMAC (MPa)			PDMS-TBHDPB (MPa)			PDMS-4CBTBPB (MPa)		
		3%	5%	10%	3%	5%	10%	3%	5%	10%
1	2.52	6.27	3.96	2.59	1.44	1.35	3.03	1.81	2.21	2.14
2.13	2.22	6.73	3.55	3.19	1.90	1.83	3.60	2.24	2.65	2.64
4.54	1.98	7.18	3.13	3.73	2.21	2.30	4.15	2.63	3.13	3.11
9.68	1.94	7.21	3.14	3.91	2.27	2.40	4.30	2.65	3.10	3.17
44.01	10.60	13.11	13.42	4.54	7.53	7.39	5.76	6.96	6.47	6.29
93.82	43.35	32.14	50.84	34.56	41.7	41.4	38.9	40.66	39.4	40.2
200	229.36	222.10	264.15	211.78	226	233	237	234	235	232

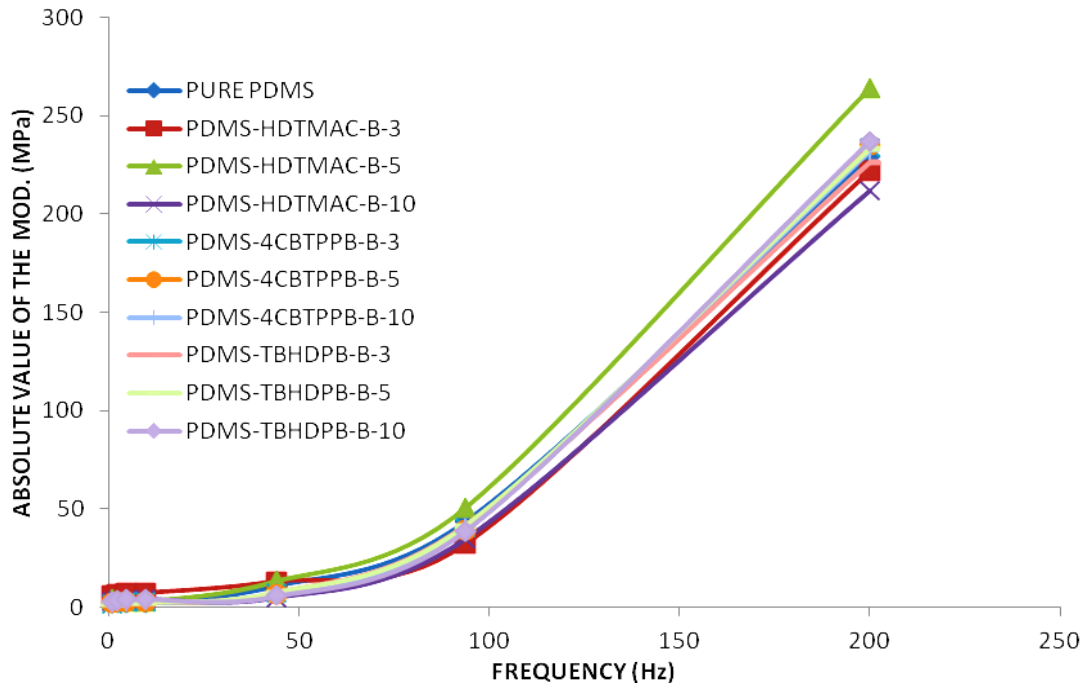


Figure 4.19 : Frequency versus absolute value of the modulus ($|E|$) results of PDMSNCs

At low frequencies E' is very low, because the most of the deformation comes from the viscous part of the material. The absolute value of the modulus is equal to E' at high frequencies. Because at high frequencies, there is not enough time for any appreciable flow to occur in the viscous part of the viscoelastic material during the time of a cycle of oscillation. The motion is due to the stretching of the elastic part of

the viscoelastic material, so the dynamic modulus (E') is equal to the modulus of the elastic part [52].

According to DMA test results of the PDMSNCs, it can be seen that the samples are supporting the viscoelastic material behavior.

4.6 Hardness Test Results

The hardness measurements were made with a Zwick Roell Shore A measuring apparatus. A steel indenter is pushed against the material and the depth to which it penetrates is a measurement of hardness. Hardness is a rough but rapid method of characterizing a material and, although it is of a doubtful nature, is widely used in the rubber industry. Because elastomer materials relax and decrease their stress over time, the measurement can be slightly difficult to interpret. All measurements of hardness in this report were made 3 s after the indenter had been pushed down into the material.

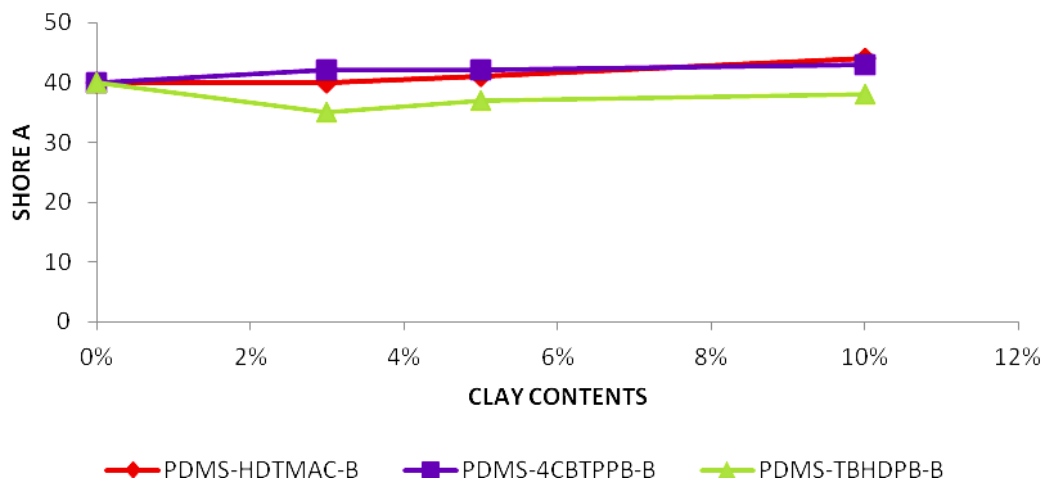


Figure 4.20 : Hardness test results of the PDMS/organoclay nanocomposite with varied organoclay content

According to the Figure 4.20 it can be seen that PDMS-HDTMAC-B the hardness was increased with very low acceleration and it can be accepted as hardness wasn't change by the increased clay content.

4.7 Contact Angle Test Results

Figure 4.21 shows the contact angles for water on the cross-linked pure PDMS and PDMSNC at increasing clay contents.

The water contact angle value of the cross-linked pure PDMS is obtained as 104.1° . Water contact angle values of PDMSNCs prepared with HDTMACmodified bentonite show no appreciable change with increasing clay content. On the contrast, water contact angle values of PDMSNCs prepared with TBHDPB and 4CBTPPB modified bentonite are decreasing with increasing organoclay contents from 104.1° to 92.3° and 81.1° respectively. Clays' hydrophilicity is decline of the water contact angle values are lower than PDMS. According to literature if water contact angle of a material is lower than 90° that can be accepted as hydrophilic material. Therefore, water contact angle of the PDMS could be decreased by adding hydrophilic clays.

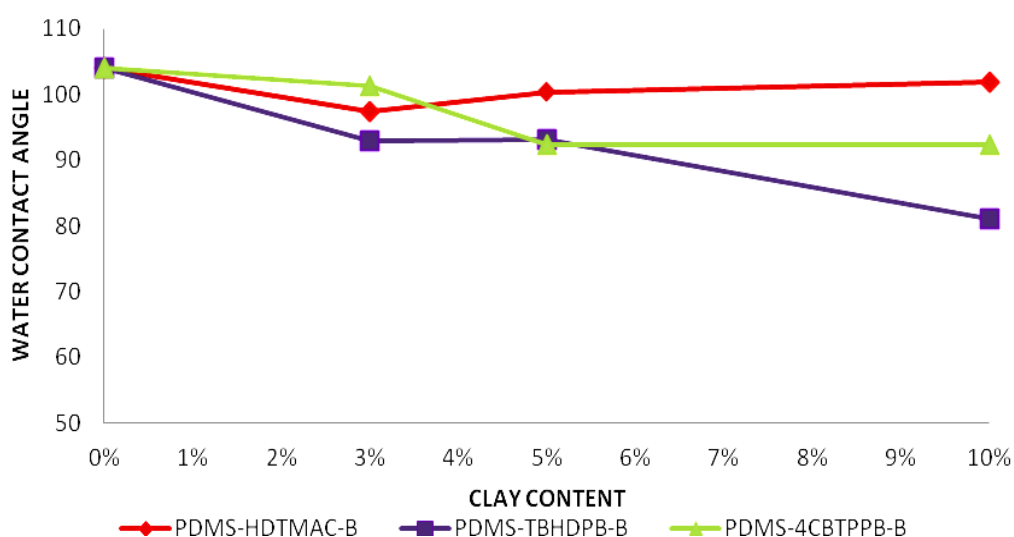


Figure 4.21: Water contact angle results of the pure PDMS and PDMSNCs

Surface free energies of the samples were calculated from the related equations which are given as Eq. 3.1, Eq. 3.2 and Eq. 3.3. While surface free energy values of PDMS-HDTMAC-B and PDMS-4CBTPPB-B have no appreciable change, values of PDMS-TBHDPB-B were increased from $14,4 \text{ mJ/m}^2$ to $21,3 \text{ mJ/m}^2$ according to Figure 4.22.

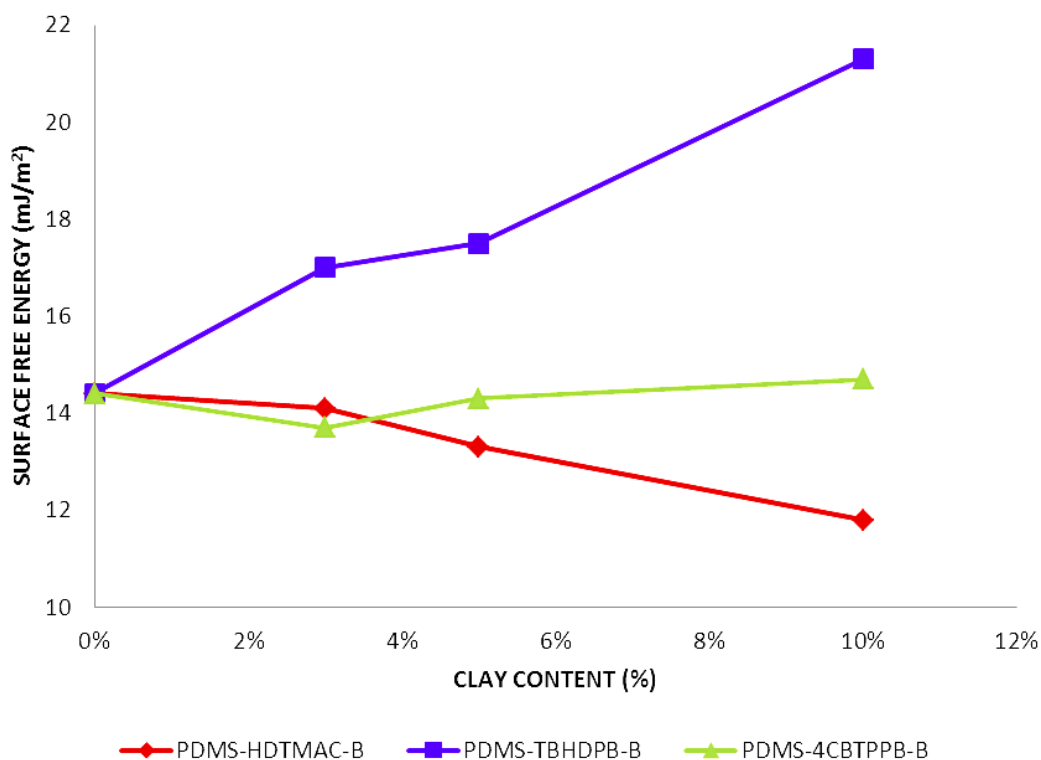


Figure 4.22: Surface free energy results of the pure PDMS and PDMSNCs

4.8 FE-SEM Test Results

Field Emission Scanning Electron Microscopy was used to examine the morphology of the fractured samples by applying carbon coatings. The distributions of P (phosphorus) in PDMS nanocomposite (prepared by phosphonium salt modified bentonites) samples were investigated by the mapping results obtained from SEM-EDX analysis. Red points in the FE-SEM images represent the P atoms (Figure 4.23 and Figure 4.24). Due to the FE-SEM results were supporting the XRD results of the PDMSNCs that can be said exfoliated structure was obtained. Beside this that can be seen from the FE-SEM pictures diameters of the red points are about 400 nm. Due to one dimension is nanometer size at least, nanocomposite were obtained.

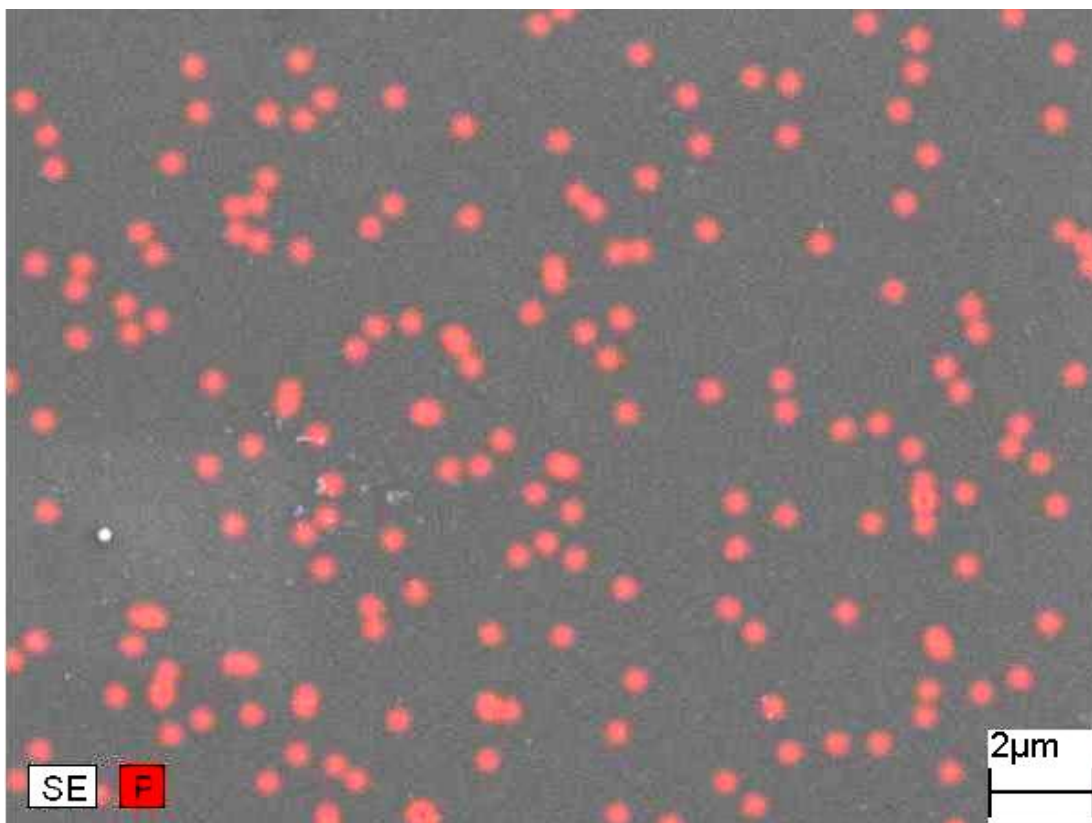


Figure 4.23 : FE-SEM image of PDMS-4CBTPPB-B-5

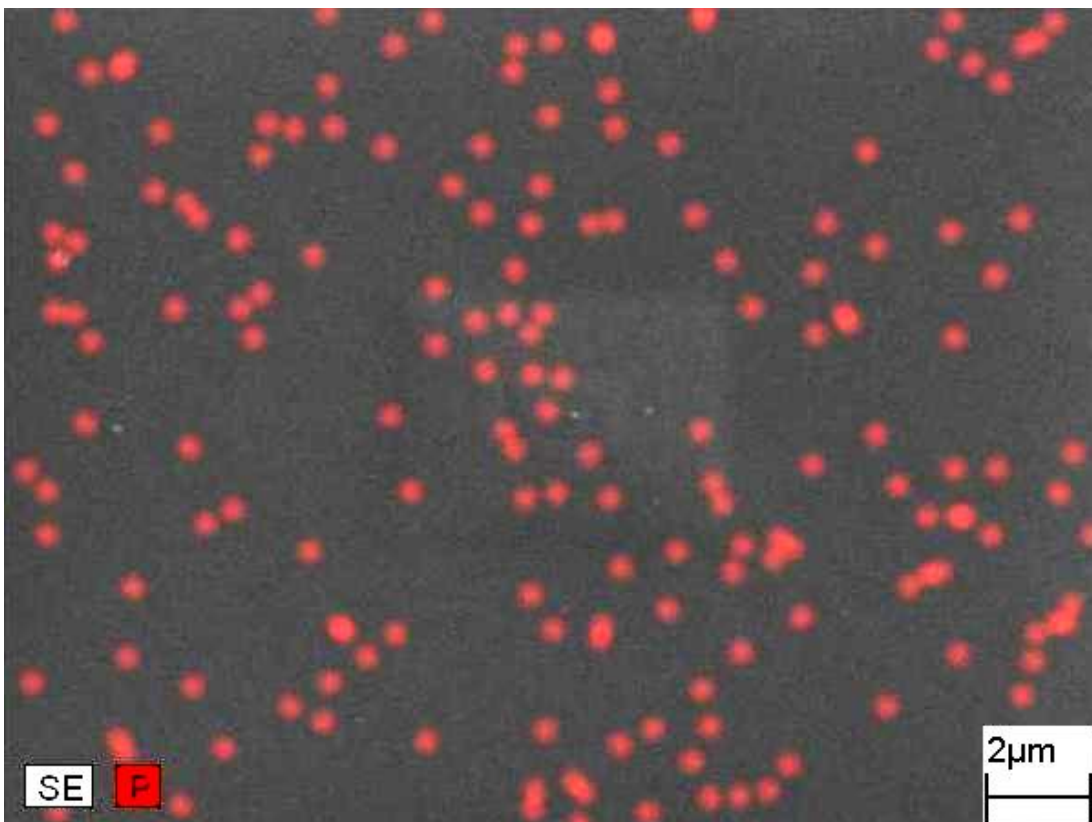


Figure 4.24: FE-SEM image of PDMS-TBHDPPB-B-5

5. CONCLUSIONS

In this study, cross-linked PDMS nanocomposites were successfully prepared by using alkyl ammonium or alkyl phosphonium modified bentonites at varying compositions (3-5-10%). The modification of bentonite was carried out in house. The used crosslinker agent was dicumyl peroxide (DCP). Ultrasonication assisted solution intercalation and subsequent in-situ polymerization method was implemented.

FTIR analysis showed the lacking of any chemical interaction between the organically modified bentonite and the PDMS. XRD results exhibited the 40-45% intercalation of raw bentonite with hexadecyltrimethylammonium chloride (HDTMAC), tributylhexadecylphosphonium bromide (TBHDPB) and (4-carboxybutyl)triphenylphosphonium bromide (4CBTPPB). XRD patterns of PDMS/organoclay nanocomposites did not showed any diffraction peaks due to the possible exfoliation. FE-SEM results supported the XRD results showing the nanometer level dispersion of organoclays in the PDMS nanocomposite systems.

It was revealed from TGA analysis that the onset decomposition temperatures of pure PDMS increased by the addition of organoclays. The decomposition temperatures of PDMS-4CBTPPB-B nanocomposites were found to be improved with respect to PDMS-HDTMAC-B and PDMS-TBHDPB-B nanocomposites due to the existing phenyl groups in the structures.

Tensile test results showed that the significant improvement in elastic modulus was obtained in 5 and 10% organoclay content for all type of PDMS nanocomposites. PDMS nanocomposites prepared with HDTMAC modified bentonites exhibited better properties in comparison to the others. Dynamic mechanical analysis results supported this finding.

Contact angle test results showed that; the PDMS/organoclay nanocomposites prepared with TBHDPB-B causes in surface hydrophilicity due to decrease of water

contact angle from 104° to 81,1° for the comparison to pure PDMS, while the other type of nanocomposites had no significant change.

Finally, PDMSs have been traditionally reinforced with silica in industrial applications. Agglomeration of the silica particles is a general problem often prevents full realization of the filler capability. It is believed that due to the improved thermal stability and mechanical properties, organoclay based PDMS nanocomposites can be used in industrial applications instead of silica, especially when the weight reduction is priority.

REFERENCES

- [1] **Hull, D.**,(1981) *An Introduction to Composite Materials*, Cambridge: Cambridge University Press
- [2] **Callister, J., and William D.**, (2003). *Materials Science and Engineering: An Introduction*. 6th ed., New York: John Wiley & Sons.
- [3] **Harper, C.A.**, (2002). *Handbook of Plastics, Elastomers & Composites*. 4th edition: McGraw-Hill.
- [4] **Matthews, F.L., and Rowlings R.D.**, (1994). *Composite Materials, Engineering & Science*, London, New York: Chapman & Hall.
- [5] **Daniel, I., and Ishai O.**, (1994). *Engineering Mechanics of Composite Materials*, New York: Oxford University Press.
- [6] **Chawla, K.**, (1998). *Composite Material Science and Engineering*. 2nd ed. New York: Springer - Verlag
- [7] **Sawyer, L.C., and Grubb D.T.**, (1987). *Polymer Microscopy*, New York: Chapman and Hall.
- [8] **Rosen, S.L.**, (1982). *Fundamental Principles of Polymeric Materials*, NewYork:John Wiley &Sons.
- [9] **Ishida, H., Campbell, S., Blackwell, J.**, (2000). General Approach to Nanocomposite Preparation, *Chemistry of Materials*, **Vol. 12**, pp. 1260-1267.
- [10] **Alexandre, M., Dubios, P.** (2000). Polymer-layered silicate nanocomposites: preparation, properties, and uses of a new class of materials, *Materials Science and Engineering*, **Vol. 28**, pp. 1-63.
- [11] **Di Ventra, M., Evoy, S., Heflin, Jr., J.R.**, (2004). Introduction to Nanoscale Science and Technology. Boston : Kluwer Academic Publishers.
- [12] **Zeng, Q., H., Yu, A., B., Lu, G., Paul, D., R.**, (2005). Clay-based polymer nanocomposites: research and commercial development, *Journal of Nanoscience and Nanotechnology*, **Vol. 5**, pp. 1574-1592.
- [13] **Pinnavaia, T. J., Beall G. W.**, (2000). *Polymer-Clay Nanocomposites*, England: John Wiley & Sons.
- [14] **Moore, D.M., Reynolds R.C.**, (1997). *X-ray Diffraction and the Identification and Analysis of Clay Analysis of Clay Minerals*, Oxford: OxfordUniversity Press.

- [15] **Alexandre, M., Dubois P.**, (2000). *Polymer-Layered Silicate Nanocomposites: Preparation, Properties, and Uses of a New Class of Materials.* Materials Science and Engineering, **Vol. 28**: p. 1-63.
- [16] **Deraj, R.N., and Guy, R.D.**, (1981). *Clays and Clay Min.*, **Vol.29**, pp. 205-212.
- [17] **Lagaly, G.**, (1986). Colloids in Ullmann's Encyclopedia of Industrial Chemistry, pp. **Vol A7**.
- [18] **Bayram, H., Onal, M., Yilmaz, H., Sarıkaya, Y.**, (2010). Thermal Analysis of a White Calcium Bentonite, *Journal of Thermal Analysis and Calorim*, **Vol.101**, pp. 871-879.
- [19] **Utracki, L., A.**, (2004). Clay-Containing Polymeric Nanocomposites. Shropshire : Rapra Technology Limited, p. 1st Edition
- [20] **Bergaya, F., Lagaly, G.**, (2001). Surface modification of clay minerals.. *Applied Clay Science : s.n.*, **Vol. 19**, pp. 1-3.
- [21] **Lan, T.**, (1999). Advances in Nanomer Additives for Clay/Polymer Nanocomposites. San Francisco, CA : s.n., Proceeding of Additives 99.
- [22] **LeBaron, P., C., Wang, Z., Pinnavaia, T., J.**, (1999). Polymer-layered silicate nanocomposites: an overview. *Applied Clay Science*, **Vol. 15**, pp. 11-29.
- [23] **Krishnamoorti, R., Vaia, R., Giannelis, E., P.**, (1996). Structure and dynamics of polymer-layered silicate nanocomposites. *Chemistry of Materials*, **Vol. 8**, pp. 1728-1734.
- [24] **Boccaleri, E.** Synthesis, functionalisation and charatcerisation of nanostructured materials. Torino : Università del Piemonte Orientale "A. Avogadro", *Centro Interdisciplinare NanoSiSTeMI*, July 10, 2007.
- [25] **Kornmann, X.**, (2001). Synthesis and Characterization of Thermoset-Clay Nanocomposites, *Division of Polymer Engineering*, Luleå University of Technology, Luleå, Sweden.
- [26] **Zanetti, M., Lomakina, S., Camino, G.**, (2000). Polymer layered silicate nanocomposites, *Macromolecular Materials and Engineering*, **Vol. 279**, pp. 1-9.
- [27] **Vaia, R. A., Ishii, H., Giannelis, E., P.**, (1993). Synthesis and properties of two dimensional nanostructures by direct intercalation of polymer melts in layered silicates., *Chemistry of Materials*, **Vol. 5**, pp. 1694-1696.
- [28] **Leszczyńska, A., Njuguna, J., Pielichowski, K., Banerjee, J., R.**, (2007). Polymer/montmorillonite nanocomposites with improved thermal properties Part I. Factors influencing thermal stability and mechanisms of thermal stability improvement, *Thermochimica Acta*, **Vol. 453**, pp. 75-96.
- [29] **Dennis, H., R., Hunter D., L., Chang D., Kim S., White J., L., Cho J., W., Paul D., R.**, (2001). Effect of Melt Processing Conditions On the

Extent of Exfoliation in Organoclay-Based Nanocomposites, *Polymer*, **Vol. 42**, pp. 9513-9522

- [30] **Yilgör, İ., Mcgrath, J.E.**, (1988). Polysiloxane Containing Copolymers: A Survey of Recent Developments *Adv. Polym. Sci.*, **Vol 86**, pp. 1 – 86.
- [31] **Url-1**<<http://www.mit.edu/~6.777/matprops/pdms.htm>> accessed at 25.04.2012
- [32] **Url-2**<http://www.dowcorning.com/content/publishedlit/51-960A-01.pdf> accessed at 7.12.2012
- [33] **Burnside, S.D., Giannelis, E.**, 1995. Synthesis and Properties of New Poly (Dimethylsiloxane) Nanocomposites, *Chem. Mater.*, **Vol. 7**, pp.1597-1600.
- [34] **Takeuchi, H., Cohen, C.**, 1999. Reinforcement of Poly (dimethyl siloxane) Elastomers by Chain-End Anchoring to Clay Particles, *Macromolecules*, **32**, pp. 6792-6799.
- [35] **Burnside, S., D., Giannelis, E., P.**, 2000. Nanostructure and Properties of Polysiloxane–Layered Silicate Nanocomposites, *J. Polym. Sci: Part B :Polymer Physics*, **Vol. 38**, 1595 – 1604.
- [36] **Ray, S., S., Okamoto, M.**, (2003). Polymer/layered silicate nanocomposites: a review from preparation to processing, *Progress of Polymer Science*, **Vol.28**, pp. 1539-1641
- [37] **Voulomenou, A., Tarantili, P. A.**, (2010). Preparation, Characterization, and Property Testing of Condensation-Type Silicone/Montmorillonite Nanocomposites, *Journal of Applied Polymer Science*, **Vol. 118**, p.p 2521–2529
- [38] **Shirazi, Y., Ghadimi, A., Mohammadi, T.**, (2011). Recovery of Alcohols from Water Using Poly (dimethyl siloxane)–Silica Nanocomposite Membranes: Characterization and Pervaporation Performance, *Journal of Applied Polymer Science*, **Vol. 124**, pp. 2871–2882
- [39] **Schmidt, D., F., Clément, F. and Giannelis, E., P.**, (2006). On The Origins of Silicate Dispersion in Polysiloxane/Layered-Silicate Nanocomposites, *Advanced Functional Materials*, **Vol.16**, pp. 417-425.
- [40] **Lassen, C., Hansen, C., L., Mikkelsen, S., H., Maag, J.**, (2005). Siloxanes-Consumption, Toxicity and Alternatives, *Danish Ministry of the Environment*.
- [41] **Billmeyer, F.W.**, (1984). *Textbook of Polymer Science*. New York: John Wiley & Sons.
- [42] **Url-3**<<http://www.mrl.ucsb.edu/centralfacilities/x-ray/basics>> accessed at 12.12.2012
- [43] **Ray, S.S., Okamoto M.**, (2003). New Polylactide/Layered Silicate, Nanocomposites; Melt Rheology and Foam Processing, *Macromolecular Materials and Engineering*, **Vol.288**: pp. 936-944.

- [44] **Khanbabaei, G., Farahani, E., V., Rahmatpour, A.,** (2012). Pure and mixed gas CH₄ and n-C₄H₁₀ permeation in PDMS-fumed silica nanocomposite membranes, *Chemical Engineering Journal*, **Vol.191**, pp.369-377.
- [45] **Url-4** <<http://infohost.nmt.edu/~mtls/instruments/Fesem/FESEM%20principle.htm>> accessed at 19.01.2013
- [46] **Url-5** <<http://www.wcaslab.com/tech/tbftir.htm>> accessed at 19.01.2013
- [47] **Mezger, T., G.,** (2006). "The Rheology Handbook, 2nd Edition, ISBN:3-87870-174-8, pg:131.
- [48] **Silva, L., F., M., Öchsner, A., Adams, R., D.,** (2011). Handbook of Adhesion Technology, Springer, ISBN 9783642011689.
- [49] **Wei, J., Zhang, Y.,** (2012). Application of Sessile Drop Method to Determine Surface Free Energy of Asphalt and Aggregate, *Journal of Testing and Evaluation*, **Vol. 40**, No. 5.
- [50] **Zenkiewicz, M.,** (2007). Methods for the calculation of surface free energy of solids, *Journal of Achievements in Materials and Manufacturing Engineering*, **Vol. 24**, pp. 252-256.
- [51] **Chassin, P., Jounay, C., Quiquampoix, H.,** (1986). Measurement of surface free energy of calcium-montmorillonite, *Clay Minerals*, 21, pp. 899-907.
- [52] **Nielsen, L., E., Landel, R., F.,** (1994). Mechanical Properties of Polymers and Composites, Marcel Dekker, New York.
- [53] **Lewicki, J., P., Liggat, J., J., Patel, M.,** (2009). The thermal degradation behaviour of poly (dimethyl siloxane) /montmorillonite nanocomposites, *Polymer Degredation and Stability*, **Vol. 94**, pp. 1548-1557.
- [54] **Labruyere, C., Gorrasi, G., Monteverde, F., Alexandre, M., Dubois, Ph,** (2009). Transport properties of organic vapour in silicone/clay nanocomposites, *Polymer*, **Vol. 50**, pp. 3626-3637.

CURRICULUM VITAE



Name Surname: Yağmur ÇAVUŞOĞLU

Place and Date of Birth: İzmir-18.05.1987

Address: Nazım Hikmet Bulvarı C4 Blok D:83 INNOVIA2 Sitesi

Esenyurt / İSTANBUL

E-mail: ycavusoglu@itu.edu.tr / yagmur.cavusoglu@hotmail.com

B.Sc.: Kocaeli University – Chemical Engineering

M.Sc.: Istanbul Technical University – Polymer Science and Technology

PRESENTATIONS ON THE THESIS

Çavuşoğlu, Y., Özkoç, G., Uyanık, N., “Synthesis and Characterization Of CrossLinked Poly (dimethyl siloxane) Nanocomposites” *1st International Plastic and Rubber Technologies Symposium and Product Exhibition*, May 29-31, 2013, Ankara, Turkey.

